



A mathematical model for predicting complete compressive stress-strain curve of plain and short fiber reinforced clay adobes

F. Faghih-Khorasani¹, M. Zaman-Kabir¹, Kh. Ghavami²

¹ Department of Civil and Environmental Engineering, Amirkabir University of Technology, Tehran, Iran

² Department of Civil Engineering, Pontificia Universidade Catolica do Rio de Janeiro, Brazil

ABSTRACT: Following the principles of low-cost, energy-saving, low polluting, and sufficient thermal, humidity and acoustic insulation of soil blocks as a construction material, there is an increasing interest to study clay adobe elements. This study presents a mathematical model for predicting the relationship between uniaxial compressive stress and corresponding strain which can be useful for simulating the structural behavior of plain and short fiber reinforced adobes with concrete damage plasticity model in ABAQUS. In this direction, the compressive properties of four different plain and short fiber reinforced adobes were measured in experimental tests. From the obtained results, the essential parameters of the stress-strain curves for all various mix design specimens were extracted for numerical modeling. By a statistical study on the various results of compressive tests as available in the related literature, the proposed equations were developed for predicting the necessary parameters when the only needed experimentally determined parameter is the peak compressive stress. The suggested model is compatible with the behavior of different adobes with different compositions, compacting, curing, and testing condition. The recommended model and formulations are to some extent more successful in predicting the linear and nonlinear behavior of different adobes according to other models. Finally, a mathematical model is developed for predicting the inelastic range of the compressive stress-strain curve.

Review History:

Received: Nov. 16, 2019

Revised: May. 01, 2020

Accepted: Jun. 03, 2020

Available Online: Jan. 25, 2021

Keywords:

Compressive Stress-strain

Relationship

Toughness

Mathematical Model

Clay Adobe

Fiber Reinforced Clay Adobe

1- Introduction

Sun-dried molded mud which is named adobe is one of the first least polluting and low-cost construction materials with sufficient acoustic and thermal insulation. For reducing the adobes' shrinkage and cracks, some different short randomly distributed fibers were added to their mix-design. Lack of knowledge on the complex behavior of adobe elements causes a limitation of their innovative applications. Nevertheless, the numerical simulations can provide information on the structural behavior of materials. The most important part of the simulation is the mathematical description of the real behavior which leads to the relationship between stress and strain, generating the material constitutive law. Adobe is a heterogeneous composite material whose strength is strongly affected by its composition, compacting type, curing, and also testing condition. It is not a perfectly elastic material and does not strictly follow Hooke's law, it is a quasi-brittle material, and the size of the tested specimen and the rate of applying load influence the experimental results. Examining the adobes compression experimental results within the context of engineering design also show that regardless of the specimens' shape and type of examining, there are considerable variations in ultimate compressive bearing capacity and deformation capacity due to inherent non-homogeneity and randomness of adobes arising from their non-industrialized production methods

*Corresponding author's email: mzkabir@aut.ac.ir

mix design [1,2,3,4,5]. The shape of the stress-strain curve is very complex. As it was mentioned adobe is a quasi-brittle material like concrete: although the plastic deformation is negligible, the size of the nonlinear region is large enough to be taken into account and an elastic analysis is very limited for them [6]. One of the suitable material models which can define both plasticity and damage behavior of quasi-brittle materials to simulate correctly both ascending and descending parts of stress-strain relationship is concrete damage plasticity model as described in ABAQUS software [7,8,9]. In the current study, by simulating the performed compression experiments, it was found that the required parameters to have an adequate simulation are σ_{Cp} , ϵ_{Cp} , σ_{C0} , ϵ_{C0} , E_{0c} , ϵ_{cu} . (where σ_{Cp} is the peak compressive strength, ϵ_{Cp} is the axial strain at peak compressive strength, σ_{C0} and ϵ_{C0} are the compressive strength and its corresponding strain at the point with maximum Young's modulus and E_{0c} is the maximum compressive Young's modulus, ϵ_{cu} is the ultimate strain). Nevertheless, a proper compression stress-strain curve equation should meet the following conditions [10]:

- 1- The equation should compare favorably with carefully conducted experiment results,
- 2- Both ascending and descending branches should be shown,



3-It should be established on mechanical parameters that can be experimentally determined and at the point of origin:

$$\frac{d(f)}{d\varepsilon} = E_0 \quad \text{and at the point of maximum stress: } \frac{d(f)}{d\varepsilon} = 0.$$

where f is the adobe stress, ε is its strain and E_0 is the

initial (undamaged) Young's modulus.

The present work tries to show a simple way to calculate the desired mechanical parameters for complete compressive stress-strain curve prediction when the only needed experimentally determined parameter is the maximum compressive stress which is attained easily. Having more reliable and acceptable conclusions, it was proposed to incorporate the effects of varying factors to determine the parameters of the model by collecting data from specimens with different compositions, compacting types, curing conditions, and testing conditions. It was observed that the relation between adobes' toughness and their peak stress has fewer scatters. Therefore, it was trying to evaluate toughness for the selected adobes' compression stress-strain curves and produce some equations to estimate the desired parameters for predicting the complete adobes' compression stress-strain curves. To assess desired formulations, a regression analysis was performed using the software Curve-Expert Professional 1.6.5. Some researchers proposed different stress-strain relations for adobe materials subjected to compressive loading through different methods when the needed experimentally determined parameters are both maximum compressive stress and its corresponding strain and also they do not pay attention to the required parameters for an adequate simulation by a software [1, 5, 11].

This study considers four different design mixes to study the mechanical properties of plain and short fiber reinforced adobes. For each mix design, the compressive behavior was investigated experimentally and numerically. The constitutive relation of the material for tested specimens established in compression and tensile, applying the concrete damage plasticity in the software of Abaqus. By verifying the numerical results with experimental measurements, the essential parameters were determining. After that, it was trying to proposed equations for calculating these parameters when the only needed experimentally determined parameter is maximum compressive stress, by approving that material toughness can represent the behavior of materials. In the end a mathematical model was developed for complete, both ascending and descending branches of the compressive stress-strain curve based on experimental results of plain and short fibers reinforced adobes with a different arrangement, compacting, curing, and testing condition according to this study and the literature. Finally, the suggested model was used to predict the stress-strain curves of the collected literature experiments and compare them against their experimental results when some other researcher's model predictions are presented too

2- Materials and Methods

For this study, the soil for preparing adobes was collected from the saline clay resources of Yazd-Maybod in the central region of Iran, which traditionally is used for producing burnt clay bricks. The only available water for the mixture was the salty water of Maybod. As reinforcement, straw, tire, and carpet fibers from factories in the region were used. The mechanical characteristics of the fibers are given in Table 1. Fibers were randomly cut with a length of less than 50mm and added in the proportion of 10% (wet fiber volume/ wet soil volume). The particle size distribution of the consumed soil was obtained by sieving tests (for particle sizes greater than 75 μm). A sieve analysis was carried out according to ASTM D 2487- 98 standard [12] and provided the following percentages by weight: 85.61% clay+ silt (grain diameter (dg) < 0.075 mm), 14.15% sand (0.075 mm<dg<4.75 mm), and 0.24% gravel (4.75 mm<dg<75 mm). The Atterberg limits were measured according to ASTM D4318 [13] as follows: plastic limit 25; liquid limit 43; and plasticity index 18.

For the brick preparation, water was added to the powdered soil in the proportion of 25% (water weight/dried soil weight) and allowed to soak for 24 hours. The fibers were separately added to the prepared mud in the proportion of 10% (volumetric). To produce adobes by quality-controlled industrialized procedures rather than empirical methods, the mixture of soil, water, and randomly oriented fibers were poured into the extruder machine to make adobe ingots with 100 × 100 mm² sections which were then cut into lengths of 500 mm. To minimize the shrinkage cracks, the adobe ingots were laid on two parallel narrow flat colored wooden sheets to be cured for seven days in ovens using a combined action of air and heat at about 50 °C, ceasing when the reduction of ingots' weight stopped and it got stabilized. Pictures of the extruder machine and fibers used are presented in Fig.1.

As can be seen in Table 1, the water absorption of straw fibers is very high which can be both harmful and beneficial. Saturated fibers can act as a water tank and pump the water to the binder matrix and reduce shrinkage. However, in the short term, if the fibers were not completely saturated, a high absorption coefficient may create difficulties according to the mobilization of a large part of the mixing water to the fibers during the implementation of the mixture.

3- Experimental program

Due to the lack of accessible local and international testing standards, referring especially to adobe, the size, and form of the test specimens were selected according to the masonry compressive specimens testing standards in the Eurocode 6 [15]. For compressive strength of masonry units, Eurocode 6 considers a normalized mean compressive strength which is equal to the standard compressive strength in the direction of the applied load multiplied by an appropriate shape/size ratio. A 100 * 100 * 100 mm³ cubic specimen with solid platens is used to determine the normalized compressive strength. Using the normalized compressive strength minimizes the effects of the platen restraint and shape/size of the specimen [15].

Table 1. Mechanical characteristics of reinforcing fibres [14]

Property	Unit	Tire Fibers	Carpet Fibers	Straw Fibers
		Values	Values	Values
Equivalent diameter	mm	0.80	0.45	0.3
Length	mm	10-30	10-40	10-40
Tensile strength	MPa	600	400	14.7
Elongation at break	%	22	30	1.5
Elastic modulus	GPa	2.7	0.9	0.07
Water absorption	%	2.5	1	300



(a)



(b)



(c)



(d)



(e)

Fig. 1. (a)The extruder machine with the spiral shaft, (b) the mould of the machine to shape the ingots section which is connected to the water source to produce smooth surface ingots, (c)short tire fibres, (d) short carpet fibres, (e) short straw fibres

Specimens were cut from adobe ingots in dry conditions, using a fixed-base circular hacksaw, to a length of 100mm as reference (plain adobes) and fiber reinforced adobe specimens with dimensions of 100×100×100 mm³ for compression tests. It is important to mention that reinforcing fibers changed the average section area shrinkage to some extent which is shown in Table 2.

It should be noted that according to the following relationships the length of the specimens can affect the results during the initial step and before initiating failures:

$$\Delta L = \varepsilon_0 \times L \quad \text{and} \quad \frac{\Delta L}{L} = \varepsilon_0 \quad (1)$$

Where L is the initial specimen's length in line with loading direction, ΔL is the displacement of the L. ε₀ is the uniform strain of the material outside the fracture zone when it is a characteristic property of the material (which does not depend on the specimens' dimensions).

As loading increases progressively, one can write [16]:

$$\Delta L = (\varepsilon_0 \times L) + w \quad \text{and} \quad \frac{\Delta L}{L} = \varepsilon_0 + \frac{w}{L} \quad (2)$$

Where w is the length of the fracture zone in line with loading direction and the cracks were initiated and developed.

Therefore, by starting the damage configuration, the $\frac{\Delta L}{L}$ is not a characteristic property of the material anymore and it depends on the specimens' length (L).

Uniaxial compression tests were carried out on 3 cubic specimens for each kind of adobes. The average weights and coefficient of variation (CoV) for reinforced and reference adobes are also represented in Table 2.

3.1. Uniaxial compression tests

The compressive mechanical behaviors of adobes were characterized by displacement controlled tests when the moving head of the testing machine traveled at a constant rate of 0.6 mm/min to produce the failure of the specimens during at least thirty to ninety seconds. Cubic specimens were placed between the rigid steel plates of DARTEC-9600 (testing machine). To compensate the porosity of the specimen surfaces and minimize the transported shear forces between the adobes and rigid steel plates (as a reason of different Poisson ratios of steel and adobes under pressure) during the compression tests, two layers of Neoprene were placed between the steel plates and adobes surfaces. Minimizing shear stresses induce vertical cracks. All tests were conducted at the ambient conditions of 22°C and 55% RH. Each test was stopped when the compressive stress decreased to the residual stress level in the post-peak descending branch of the stress-strain curve. Since three derived force-displacement, and stress-strain curves for each kind of adobe did not reveal significant scatters in compressive behaviors, the average compressive force-displacement and average stress-strain curves were selected as the compressive behavior for different kinds of specimens. The average compressive stress-strain curves are presented in Figure 3. In the presented curves, the updated

stress and strain are attainable as:

$$\sigma_T = \delta \left(\frac{F}{A} \right) \quad (3)$$

$$\Delta_T = \delta \left(\frac{\Delta L}{L} \right) \quad (4)$$

When σ_T is the nominal true stress, F is the momentary load, measured in each step by the testing machine, A is the momentary section area of the specimen, ε_T is the nominal axial strain, ΔL is the cumulative applied displacement that is determined by the testing machine and L is initial specimens' height. According to the so little coefficient of variance for specimens' densities in table 2, it was anticipated to do not have significant scatter in compressive behaviors for each type of adobes. It is important to remind that the median (the average of values) and characteristic (the value which is not exceeded by more than 5% of specimens) constitutive models are distinct and according to Eurocode 8 [17] characteristic properties are for linear equivalent analysis and median properties for nonlinear analysis procedures.

3.2. Acoustic Emission monitoring setting

The Acoustic Emission (AE) method is defined as the transmission of elastic waves produced by happening permanent changes in material and releasing localized internal energy, like plastic deformation, crack expansion, and other kinds of material degradation, under the loading condition [18]. Acoustic Emission occurs in discrete bursts which are named AE hits [19]. It is reasonable to assume that each AE hit is the result of the failure of a microelement [20]. For the Acoustic Emission monitoring, two transducers with a resonant frequency of approximately 150 kHz were attached to the two opposite surfaces of the specimens. According to the environmental noise level of the experiments, the threshold of the AE system detector was set to 30 dB. The other parameters were set as follows: peak definition time (PDT)= 50μs, hit definition time (HDT)= 200 μs, and hit lockout time (HLT)= 300 μs. The samples and the acoustic emission sensors were coupled with grease. The typical setup of applied AE system instrumentation which was used in this research is also presented in figure 2.

3.3. Experimental assessment

The generated compressive stress-strain curves in figure 3 can be divided into four stages: densified stage(OA), linear elastic stage(AB), weakening stage(BC), and failure stage(CD), when O is the origin of the coordinates. During the first stage, the initial existing defects by shrinkage in the adobe samples were excessively closed, therefore, the stress increases slowly, but the strain increases significantly showing densified stage. When the compressive load is applied, the soil grains shift and slip into the existing voids,

Table 2. Average area shrinkage, unit weights and coefficient of variation (CoV) for different studied adobes

	Plain adobes	Straw fibers reinforced adobes	Carpet fibers reinforced adobes	Tire fibers reinforced adobes
Average area shrinkage (%)	5.61	6.81	4.99	5.54
Difference average area shrinkage with Plain specimen (%)	-	2.2	-0.6	-0.1
Unit weight (kN/m ³)	18.24	18.02	18.20	18.32
Weight CoV(coefficient of variance)*	0.56%	0.07%	0.8%	0.47%

* $CoV = \frac{\sum(x_i - \bar{x})^2}{N}$

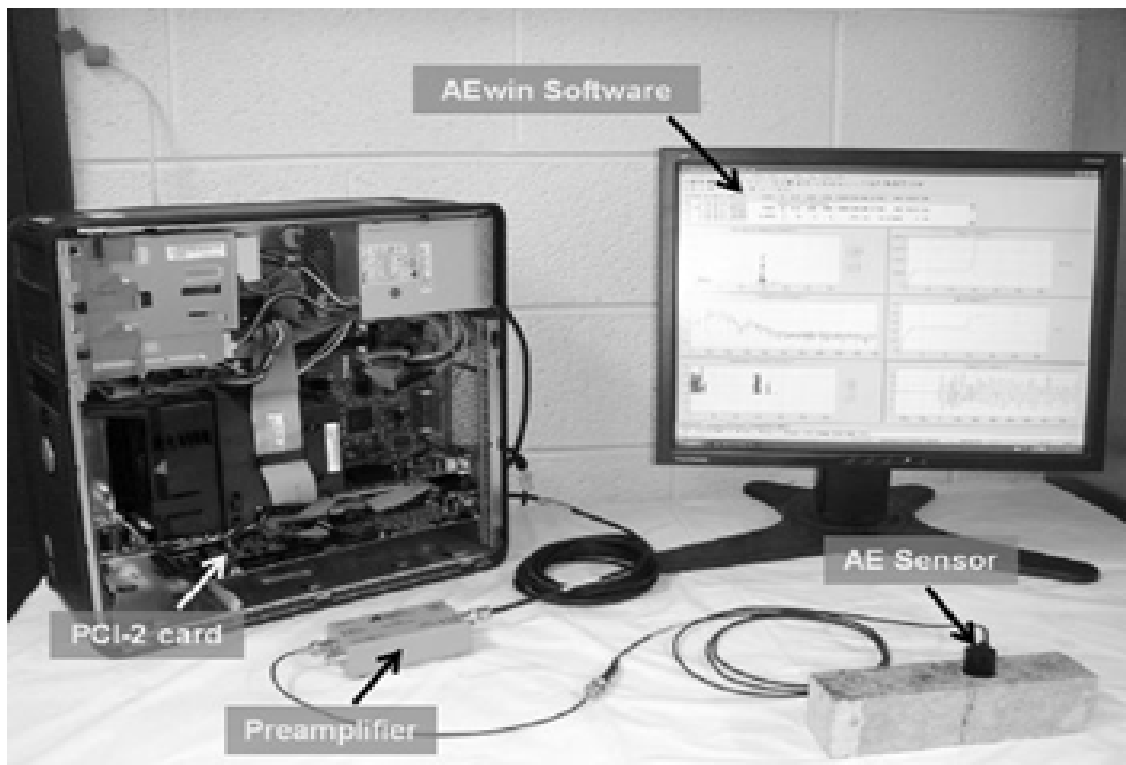


Fig. 2. The test setup of applied AE system instrumentation [20]

so the soil grains are being more compacted and densified. Subsequently, the specimen becomes stiffer and behaves as in a linear elastic stage. Before the peak load, the relation between stress and strain becomes non-linear which indicates the beginning of adobes degradation, and the adobes transit from linear elastic stage to the weakening stage. Finally, by applying more compression load, the compressive strength started to decrease slowly indicating that the sample has moved to a quasi-brittle failure mode. The mode of failure under compression for all specimens was characterized by the gradual development of several vertical cracks on the lateral sides of the specimens

The mechanical properties of different adobe specimens were illustrated in table 3 where σ_{cp} is the peak compressive strength, and ϵ_{cp} is the axial strain at peak compressive strength. σ_{c0} and ϵ_{c0} are the compressive strength and its corresponding strain at the maximum level. The maximum compressive Young's modulus was denoted

by E_{0C} ; $E_{0C} = \frac{\sigma_{c0}}{\epsilon_{c0}}$, Poisson ratio was designated by

ν ; adapted from ASTM C469M-10 [21] when ϵ_{t2} is the transverse strain at mid-height of the en and ϵ_2 is the longitudinal strain, both the stress corresponding to 40% of peak stress and this strain is to some extent equal to ϵ_{c0} . The toughness (T) was determined by integrating the stress-strain curve up to ϵ_{cu} , which is the ultimate strain corresponding to 70% of the maximum compressive stress at the downward branch or $\epsilon_{cp} + 0.02$, each one is lower [22]. The elastic toughness(ET) is calculated by integrating the stress-strain curve up to the compressive stress corresponding to the maximum Yng's modulus and the inelastic toughness was determined by integrating t stress-strain curve when the inelastic behavior was starting and Young's modulus begins to decline.

The experimental set-up for the compressive strength test and the procedures of progressing failure observations of the plain specimen is illustrated in figure 4 as (OA), (AB), (BC), and (CD) stages are defined in it. As it is shown in figure 4a, six LVDTs (Linear Variable Differential Transducer) were used in these tests, two lateral LVDTs for measuring the lateral displacements of specimens and four vertical LVDTs, two LVDTs in each side of the adobes, to measure the average vertical displacement of middle one-third of the specimens.

4- Numerical simulation of adobe elements

The numerical simulation of the experimental tests was conducted using the Abaqus/CAE 6.14-1 commercial software to numerical estimate the compressive strength and deformation of the model based on compressive and tensile experimental measurements and also to determine the essential parameters. Adobe masonry is treated as homogeneous continuous material and was simulated using the concrete damaged plasticity model. All components of the Finite Element (FE) model were discretized using 8-node 3D linear brick elements (C3D8). Loading was imposed by applying the progressive displacement. The provided

boundary conditions were imposed to have adequately simulated the experimental test setup. Uniformly distributed vertical displacements were assigned under loading regimes. The schematic loading and support conditions in Abaqus are illustrated in fig.7.

4.1. Concrete Damage Plasticity

The Concrete damage plasticity constitutive material model is based on the work of Lubliner et al. (1989) [23] and Lee and Fenves (1998) [24], where the two main failure mechanisms are the tensile cracking and the compressive crushing of the material. This model assumes that failure of the material can be effectively modeled using its uniaxial tension, uniaxial compression, and plasticity characteristics. Typical stress-strain relations in uniaxial tension and compression, assigning to materials for this model [11], are presented in Figure 5. The mathematical relationships are as follows:

$$\sigma_c = (1 - d_c) E_0 (\epsilon_c - \epsilon_c^{in}) \quad (5)$$

$$\sigma_t = (1 - d_t) E_0 (\epsilon_t - \epsilon_t^{in}) \quad (6)$$

When E_0 is the initial (undamaged) Young modulus, d_c and d_t are the scalar compression and tension damage variables respectively that account for elastic stiffness reduction, the other parameters are sho in Fig.5.

This study assumed E_0 to be the maximum of Young modulus since the adobe possesses the progressive densification and:

$$\epsilon_c^{in} = \epsilon_c - \frac{\sigma_{c0}}{E_0} \quad (7)$$

$$\epsilon_t^{in} = \epsilon_t - \frac{\sigma_t}{E_0} \quad (8)$$

$$d_c = 1 - \frac{\sigma_c}{\sigma_{cp}} \quad (9)$$

$$d_t = 1 - \frac{\sigma_t}{\sigma_{tp}} \quad (10)$$

Where, σ_{cp} is the peak compressive strength, and ϵ_{cp} is the axial strain at peak compressive strength and σ_{c0} and ϵ_{c0} are the compressive strength and corresponding strain at the point with maximum Young's modulus, respectively, as were defined in the preceding section as well. It should be noted that equation 7, σ_{c0} is considered persistent for all the points, however, equation 8, σ_t is the only quantity of tensile stress in the point which ϵ_t^{in} is calculated for.

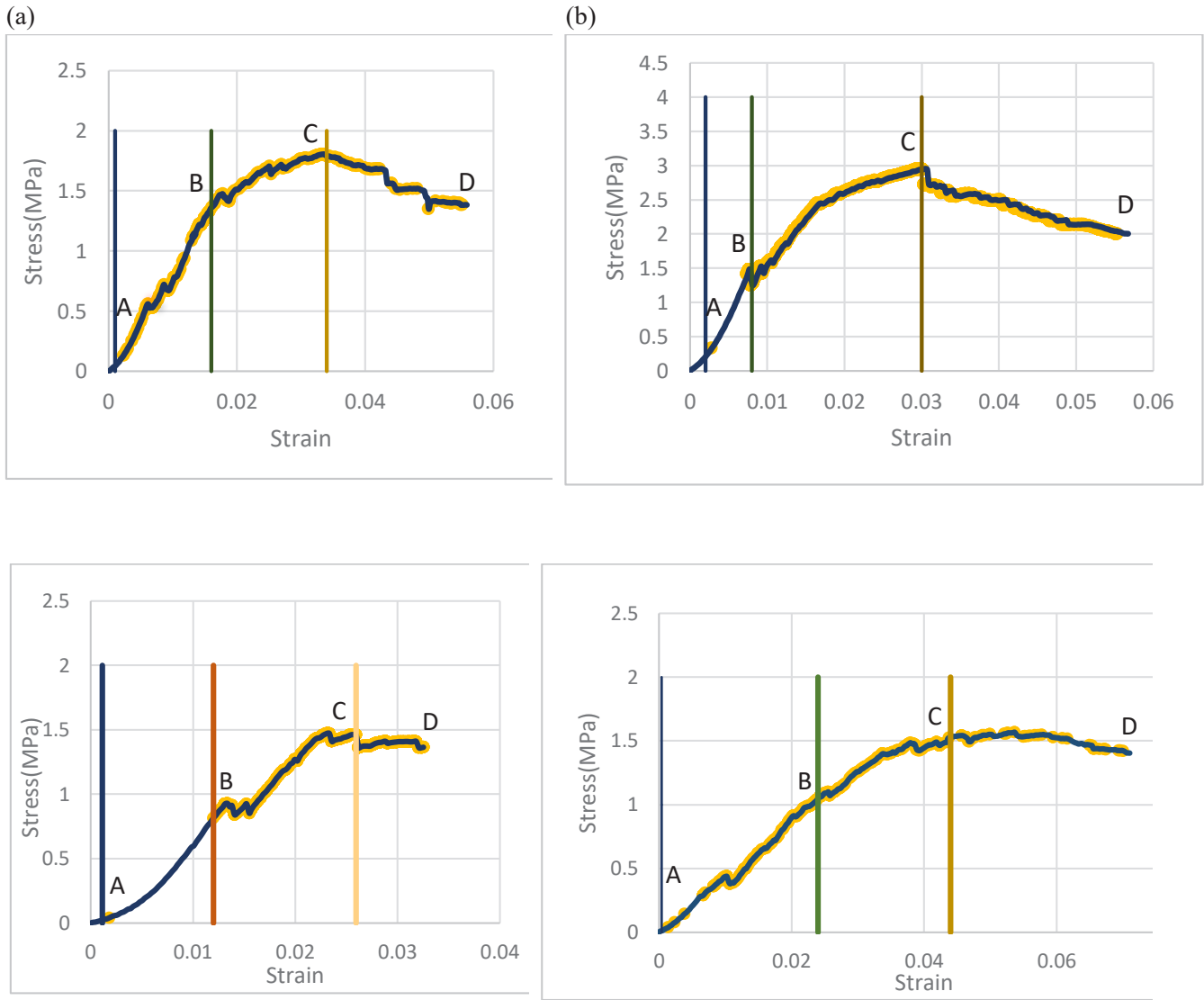
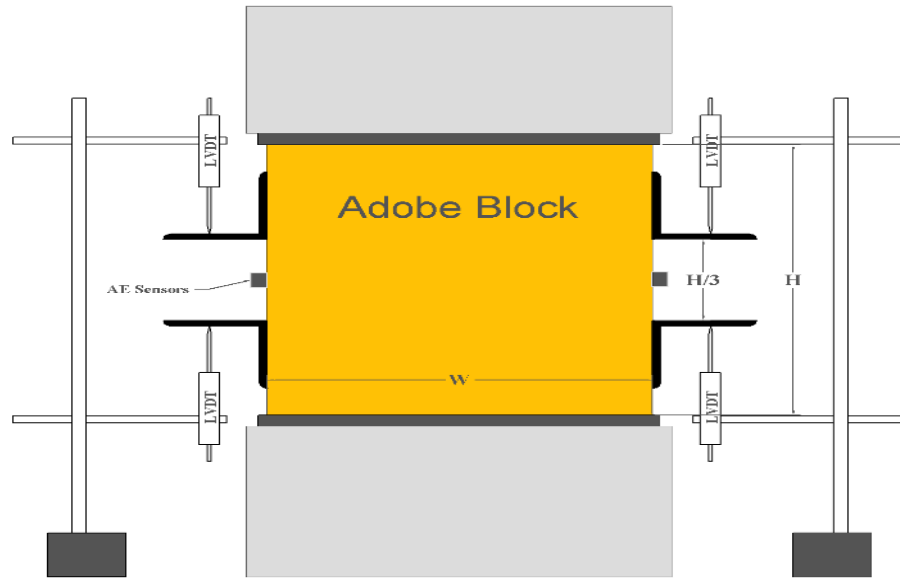


Fig. 3. The uniaxial compressive stress-strain curves, Plain specimen (a), Short Tire Fibers Reinforced specimen (b), Short Carpet Fibers Reinforced specimen (c), Short Straw Fibers Reinforced specimen (d), yellow points show the detected Acoustic hits.

Table 3. Average Mechanical properties of different reinforced adobe specimens

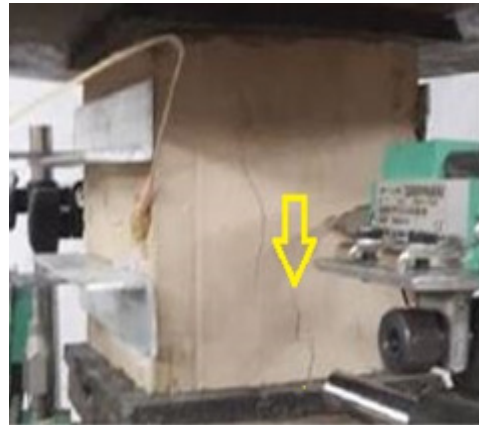
	σ_{Cp} (MPa)	ϵ_{Cp}	σ_{C0} (MPa)	ϵ_{C0}	E_{0C} (MPa)	ν	Elastic Toughness (ET) (MPa)	Inelastic Toughness from σ_{C0} to σ_{Cp}	Inelastic Toughness from σ_{Cp} to the end	Inelastic Toughness (MPa)	Toughness (T) (MPa)
Plain	1.81	0.034	1.36	0.0157	87	0.3	0.0103	0.0307	0.0323	0.0605	0.0694
Straw fibers Reinforced	1.54	0.044	1.09	0.024	45	0.3	0.0129	0.0289	0.0326	0.0593	0.0715
Carpet fibers Reinforced	1.46	0.026	0.83	0.012	71	0.2	0.0036	0.0178	0.0275	0.0434	0.0464
Tire fibers Reinforced	2.94	0.03	1.46	0.0080	183	0.2	0.0054	0.0541	0.0526	0.103	0.1108



(a)



(b)



(c)

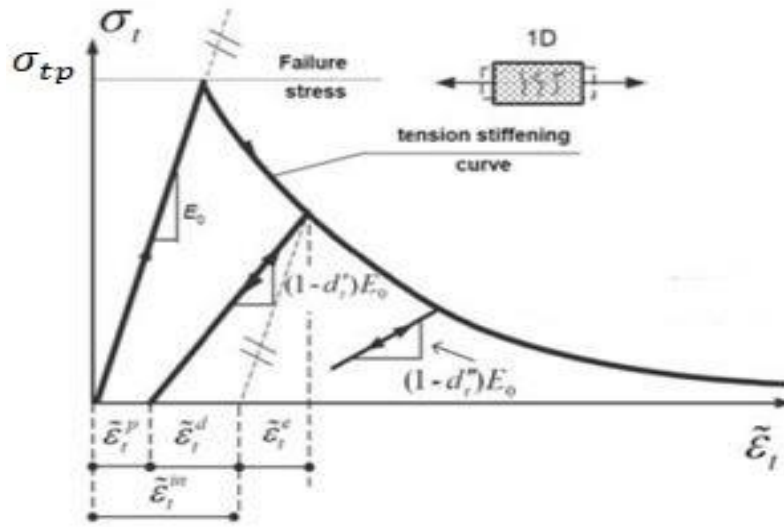


(d)

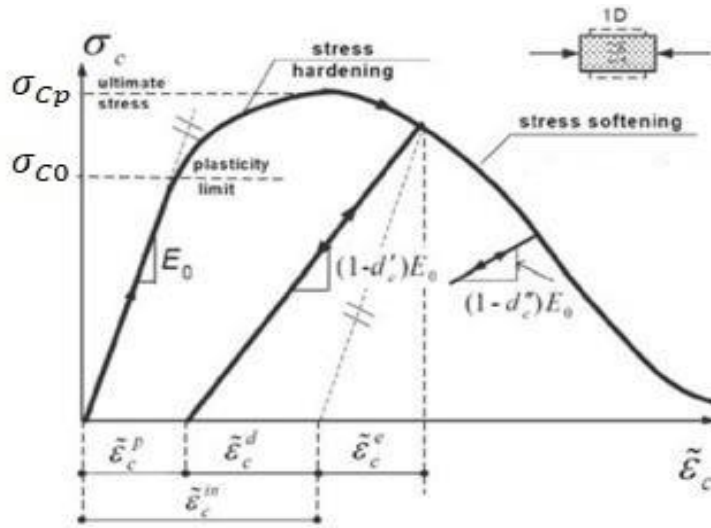


(e)

Fig. 4. (a) Compression test set-up schematic view, progressive compressive failure of one of plain specimens, (b) (OA) stage, (c) (AB) stage, (d) (BC) stage, (e) (CD) stage



(a)



(b)

Fig. 5. (a) Terms for Tension Stiffening Model and (b), for Compressive Stress-Strain Relationship [11]

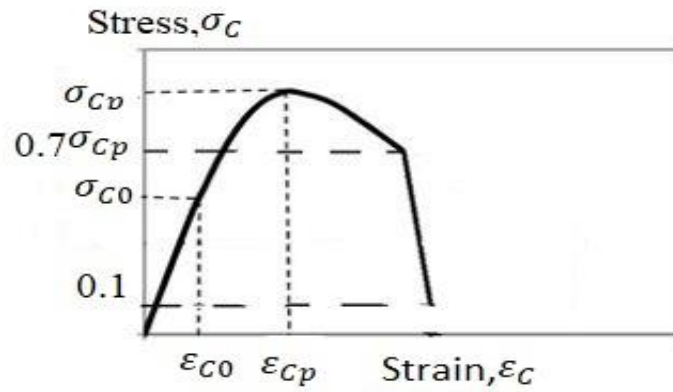
It should be noted that Abaqus checks the accuracy of the damage curve using the plastic strain values calculated as equations 11 and 12. Negative and/or decreasing plastic strain values are indicative of incorrect damage curves which may lead to generate error message before the analysis is performed [25]:

$$\epsilon_c^{pl} = \epsilon_c^{in} - \frac{d_c}{1-d_c} \frac{\sigma_c}{E_0} \quad (11)$$

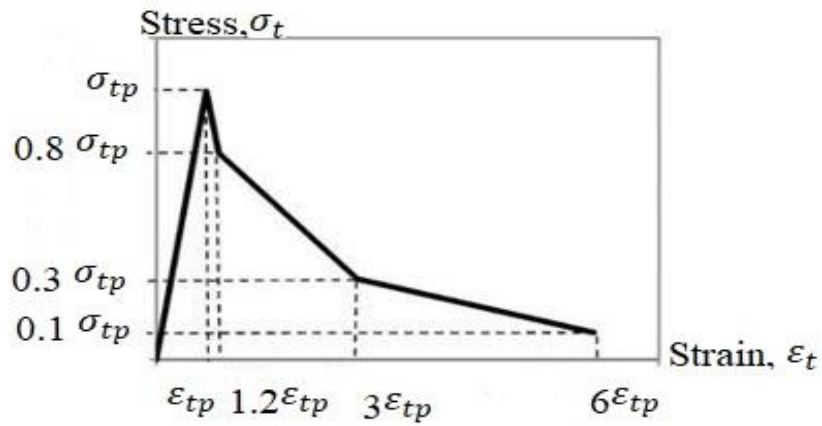
$$\epsilon_t^{pl} = \epsilon_t^{in} - \frac{d_t}{1-d_t} \frac{\sigma_t}{E_0} \quad (12)$$

4.2. Numerical Model for Stress-Strain Curve in Compression and Tension

The complete stress-strain curve for plain and short tire, carpet, and straw fibers reinforced adobes under compression and tension are derived using the results of recent experimental studies by authors, [26], when the tensile strength and properties were measured by carrying the direct tensile tests and are tabulated in Table 4, where, σ_{tp} is the peak tensile strength, ϵ_{tp} is the axial strain at peak tensile strength and E_t is the tensile Young's modulus. It should be mentioned that by direct tensile tests, it is observed that reinforcing fibers in clayey adobe prevent the tensile crack propagation after initial formation, as so-called, crack bridging role, though, prior to crack development, the fibers have no



(a)

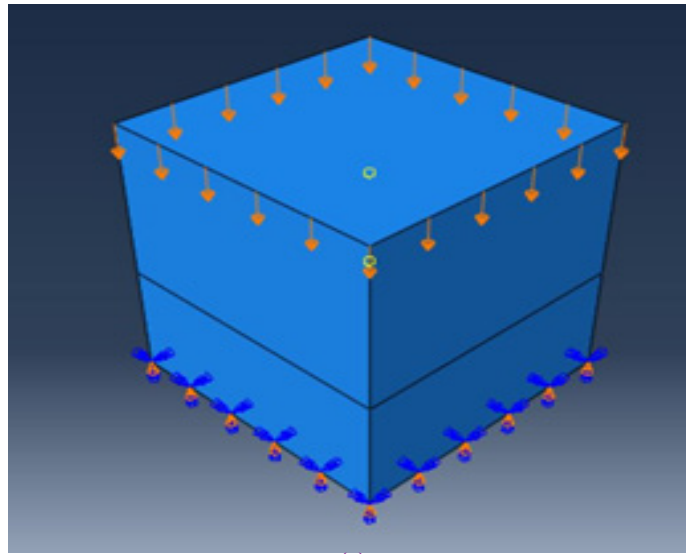


(b)

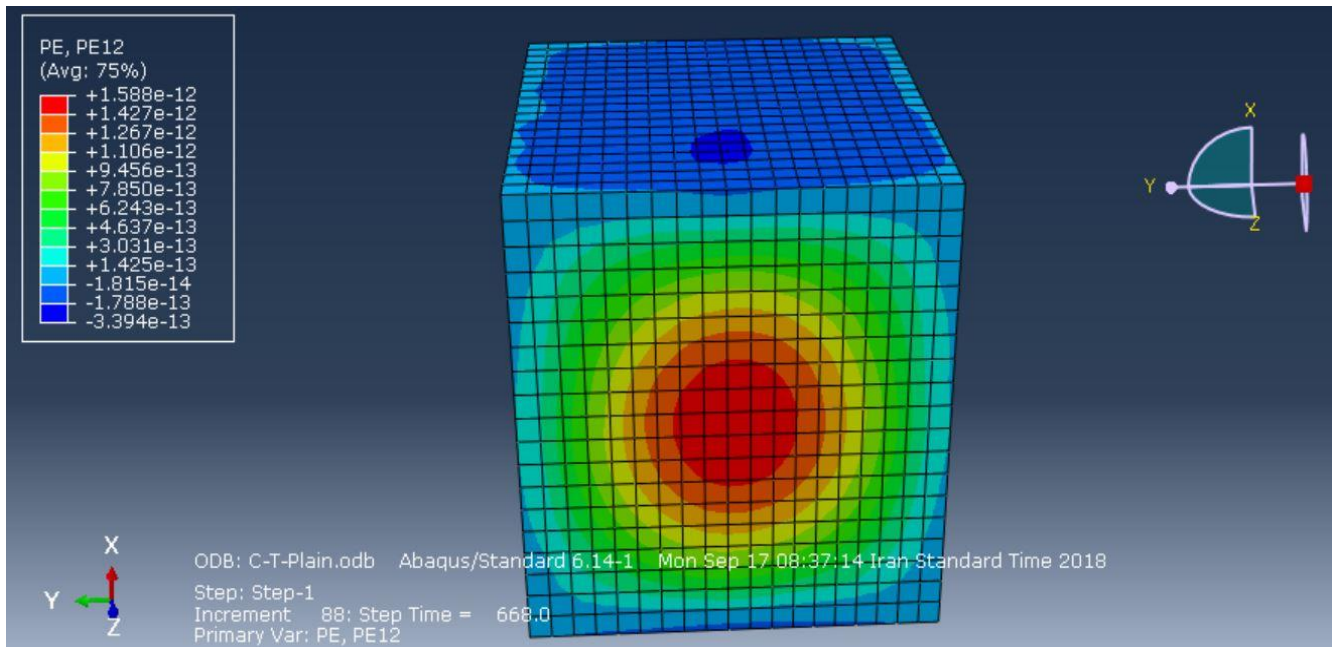
Fig. 6. Compressive Stress-Strain Relationship (a), Tensile Stress-Strain Relationship (b), for ABAQUS

Table 4. Average Mechanical properties of different reinforced adobe specimens [26]

	Direct Tensile Test		
	σ_{tp} (MPa)	ϵ_{tp}	E_t (MPa)
Plain	0.41	0.0058	70.5
Tire fibers reinforced	0.42	0.0058	72
Carpet fibers reinforced	0.41	0.0057	71
Straw fibers reinforced	0.35	0.005	70



(a)



(b)

Fig. 7. (a) Finite element model of the Compressive specimen, (b) failure state of the specimens

noticeable effect on the material behavior. The suggested modified compression and tension stress-strain relationships for presenting into ABAQUS are presented in Figure 6 when σ_0 is the point with the maximum Young modulus (E_0). Table A gives the compressive stress-strain, the values including compressive damage properties whereas table B gives the tensile stress-strain values with tensile damage properties which are presented in appendix A. Plasticity parameters are also presented in table C in appendix A.

4.3. Finite Element Modelling of the Adobe Specimens

In the numerical simulation, using ABAQUS finite element software, a general static procedure is implemented by specifying a direct method for equation solver with full Newton solution technique. Nonlinear geometrical effects are considered. All components of the Finite Element (FE) model was discretized using 8-node 3D linear brick elements (C3D8). The loading was imposed through the application of progressive displacement and the provided boundary

conditions were tried to be adequately similar to the test setup. For compressive loading, the uniform vertical displacement was applied to the top surface of the specimen. In order to have the appropriate mesh size, a mesh-dependency study was carried out and the optimum mesh in global size was obtained equal to 10 mm and the fraction of global size was considered equal to 0.1 mm. According to two different phases of the Young moduli for compressive and tensile of adobe, the FE model of cubic specimens is consists of two types of materials; lower part material with tensile Young modulus and its damage model and upper part material with compressive Young modulus and its damage model, see Figure 7, the contours of plastic strain in the direction of 12 are also displayed to indicate the damaged part of the adobe element to compare with experimental results, as was already seen in figures 4. In figure 8, stress vs. strain are presented for all plain and different fibers reinforced specimens, experimental and finite element modeling results. In the

finite element models, strains were measured at the loading points of the specimen, and stresses were calculated at the supporting points of the specimens. Since the progressive densification and stiffness increase cannot be accounted for by the concrete damage plasticity theory [11], these parts are omitted from the curves.

According to Figure 8 and 9, it is shown that the compressive strength of plain and random distributed short fibers reinforced adobe specimens are able to be estimated correctly using numerical FE simulation and the desired mechanical parameters to simulate an appropriate compressive stress-strain curve are σ_{tp} , ϵ_{tp} , E_t , σ_{cp} , E_{oc} and the ultimate strain (ϵ_{cu}), when σ_{tp} is the peak tensile strength, ϵ_{tp} is the axial strain at peak tensile strength and E_t is the tensile Young's modulus. Other parameters are explained in section 3.1 for table 3. So by this procedure, it was possible to determine desired mechanical parameters. Although the predicted elastic toughness is higher

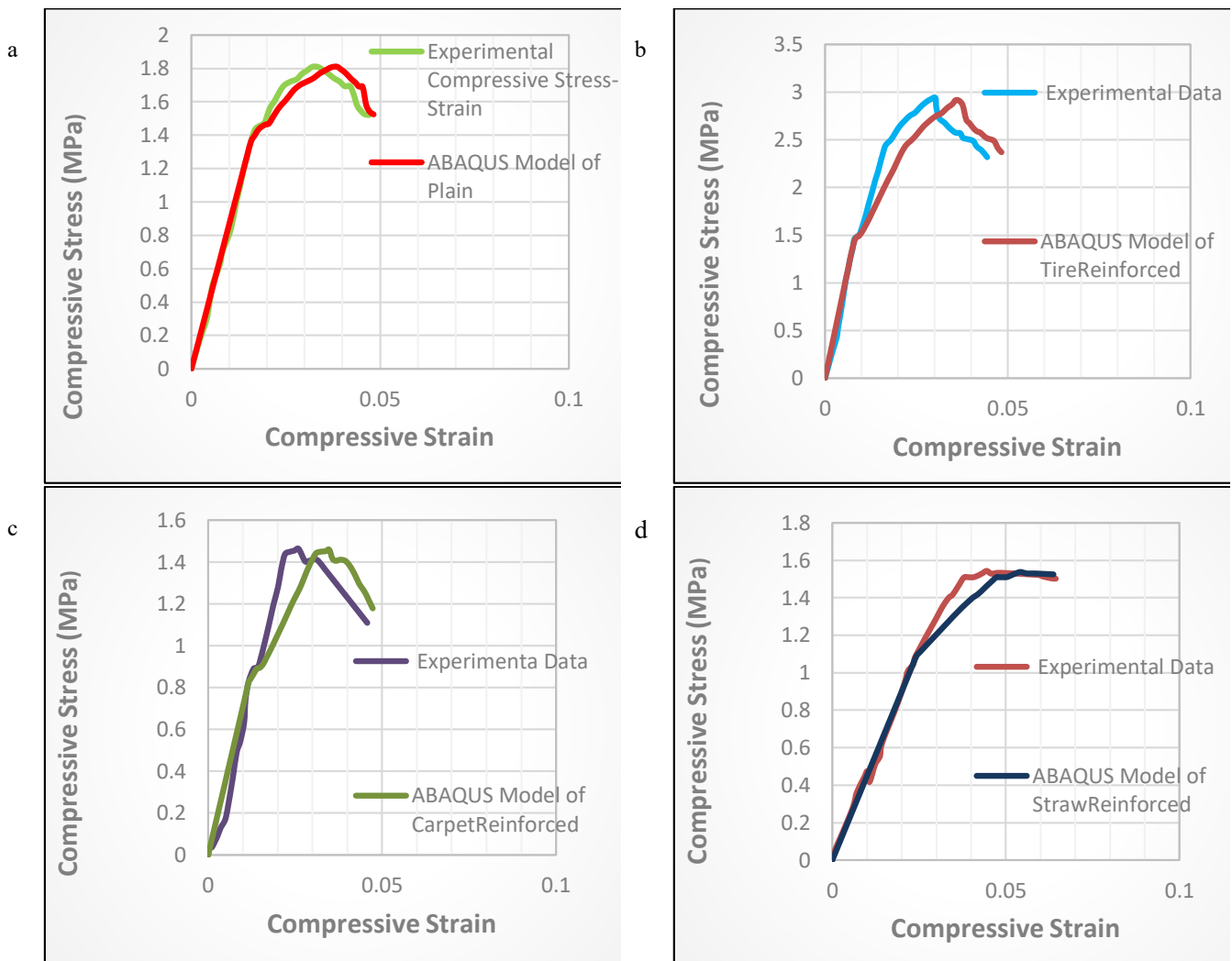
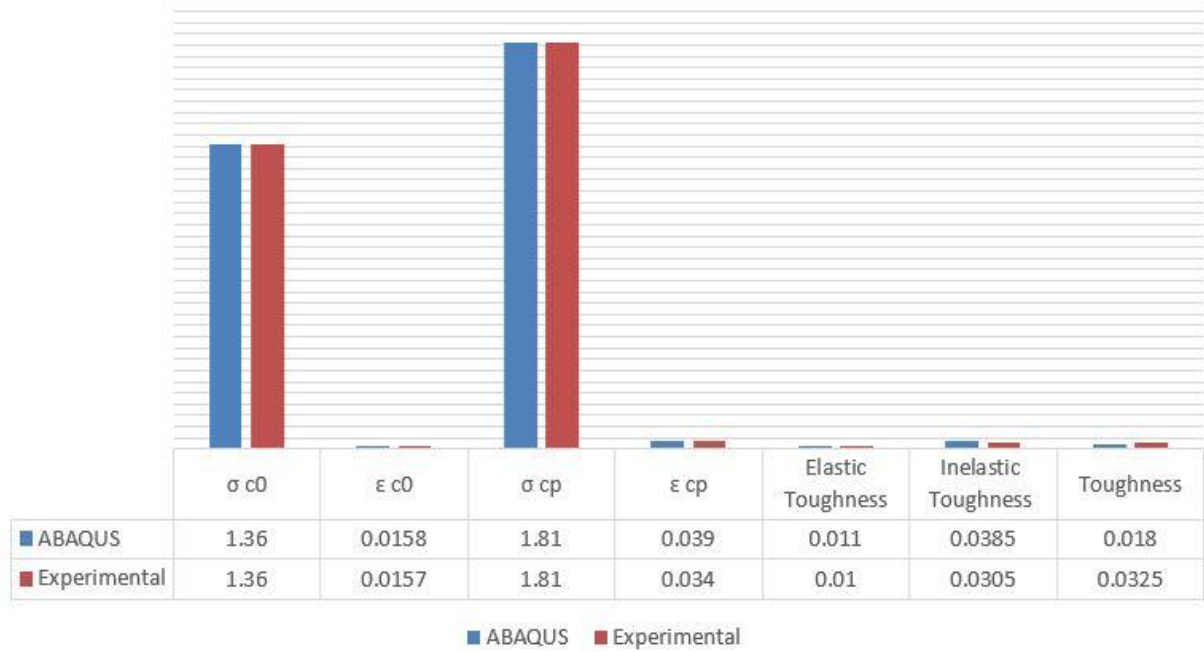


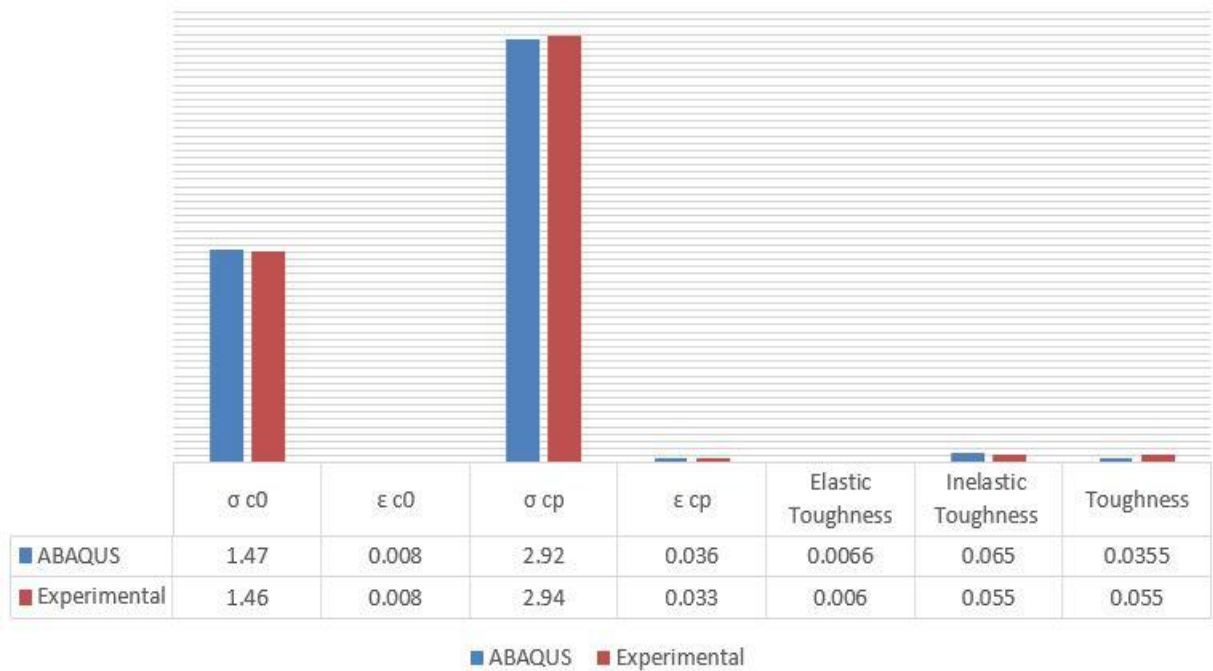
Fig. 8. Compressive stress vs. compressive strain for Plain specimen (a), Short Tire Fibers Reinforced specimen (b), Short Carpet Fibers Reinforced specimen (c), Short Straw Fibers Reinforced specimen (d).

than the experimental one because of assuming smooth line in the elastic region for FE model and also the predicted ϵ_{cp} is higher than experimental results, around +20%, however, by choosing a proper elastic Young's modulus in compression test leads to having a better correlation between experimental

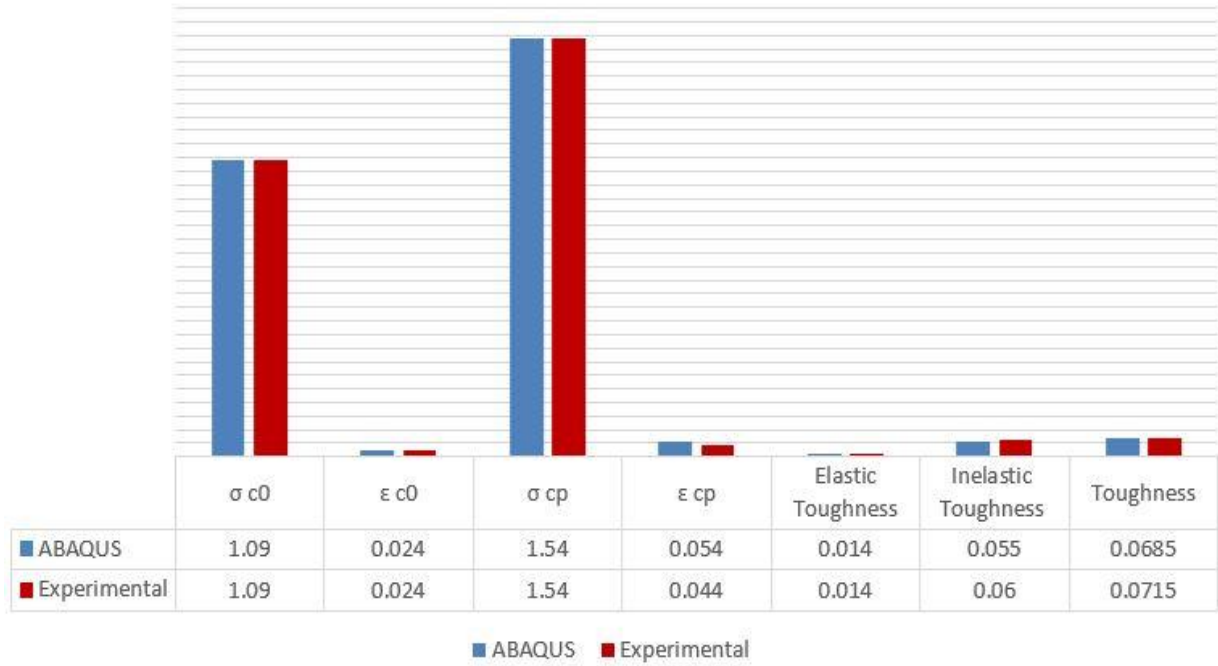
measurements and numerical results, as explained in section 3.3 and table number 3. According to equations number 7 and 11, the selected Young's modulus would affect the inelastic and plastic strains and a larger compressive elastic modulus can produce larger inelastic strains as well.



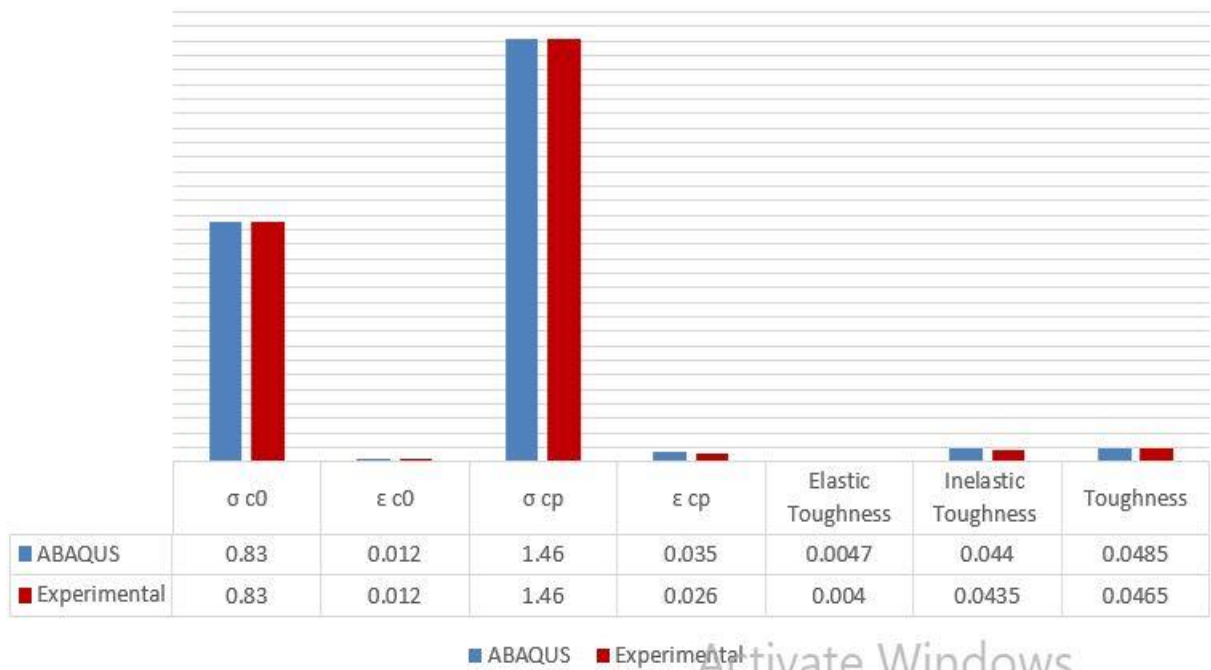
(a)



(b)



(c)



(d)

Fig. 9. A comparison between numerical results and experimental measurements of mechanical properties for (a) Plain and, (b) Tire fibres reinforced, (c) Straw fibres reinforced, (d) Carpet fibres reinforced adobe specimens.

5- Parameters estimation for compressive stress-strain curve prediction

The common analysis and design of plain or short fibers reinforced adobe structures, as quasi-brittle materials, are based on predicting the complete compressive stress-strain relationships in both ascending and descending branches. The full stress-strain path could be strongly affected by their composition, compacting type, curing circumstances. In additions, some of the testing conditions, e.g. shape and size of the specimens, strain rate, the testing machine, type of strain measurement, environmental temperature and humidity, the grain size distribution of the applied soil, type of the short reinforcing fibers, and the age of specimens are also important. The authors in their recent study proposed a new method to predict the complete compressive stress-strain relationship for plain and short fibers reinforced adobe specimens based on Acoustic Emission hits and Weibull distribution when the compressive strains are available [16]. In this section, the results of some different studies are collected in table 5 by the software of Plot Digitizer-Version 2.0, when the parameters notations are explained in sections 3.1. It should be noted that all tests have the following characters:

- All tests are carried out on new specimens to overcome different decay conditions problems,
- All the tested specimens are equal or not equal cubic (not cylindrical) specimens to prevail the effects of shape, since applying specimens in new buildings are cubic ones.
- All the tested specimens all covered by two flat layers like neoprene, flat sand, or mortar to minimize the friction between the specimens and testing machine steel plates which increase the apparent strength by decreasing lateral expansion.

One of the most important parameters in the complete stress-strain curve of adobes is the strain corresponding to the peak stress. According to table 5, it seems that adobes' strain corresponding to peak stress has a relationship with peak stress and toughness, the relation between adobes' toughness and their peak stress has fewer scatters. Therefore, it is trying to evaluate toughness for this range of data and produce some equations to estimate the desired parameters for predicting the complete stress-strain curves. In order to assess toughness for this range of data, a regression analysis was performed using the software CurveExpert Professional 1.6.5. This software makes it possible to have many equations for the fitted curves and select the most suitable one. In following the equations for predicting desired parameters and the diagrams which present the comparison between experimental data and calculated ones are presented. In the last section it was concluded that the required parameters to have an adequate software simulation are σ_{Cp} , ϵ_{Cp} , σ_{C0} , ϵ_{C0} , E_{0c} , ϵ_{cu} (where σ_{Cp} is the peak compressive strength, ϵ_{Cp} is the axial strain at peak compressive strength. σ_{C0} and ϵ_{C0} are the compressive strength and its corresponding strain at the point with maximum Young's modulus and E_{0c} is the maximum compressive Young's modulus, ϵ_{cu} is the ultimate strain).

Calculating adobes' toughness (T):

$$T = \frac{a + b\sigma_{cp}}{1 + c\sigma_{cp} + d\sigma_{cp}^2}, \quad R^2 = 0.8, \quad RMSE = 0.03 \quad (13)$$

When T is the adobe's toughness, σ_{cp} is the peak stress which is achieved experimentally, $a = 0.004$, $b = 0.008$, $c = -0.6$, $d = 0.1$,

Calculating adobes' strain corresponding to peak stress (ϵ_{cp})

$$\epsilon_{cp} = \frac{a + b\sigma_{cp} + cT}{1 + d\sigma_{cp} + eT}, \quad R^2 = 0.96, \quad RMSE = 0.004 \quad (14)$$

When ϵ_{cp} is the adobe's strain corresponding to peak stress, T is the calculated toughness, σ_{cp} is the peak stress, $a = 0.02$, $b = -0.01$, $c = 2$, $d = 2.5$, $e = 13$,

the comparison between experimental data and calculated ones for adobes' toughness and strain corresponding to peak stress versus the peak stress are presented in Fig.10.

Calculating adobes' maximum elastic modulus (E_{0c})

$$E_{0c} = \frac{a + b\sigma_{cp} + c\epsilon_{cp}}{1 + d\sigma_{cp} + e\epsilon_{cp}}, \quad R^2 = 0.6, \quad RMSE = 44 \quad (15)$$

When E_{0c} is the adobe's maximum elastic modulus, σ_{cp} is the peak stress, ϵ_{cp} is the calculated strain corresponding to the peak stress, $a = -5.7$, $b = 713$, $c = -3200$, $d = 0.8$, $e = 204$,

Calculating adobes' elastic toughness (ET):

$$ET = \frac{a + b\sigma_{cp} + cT}{1 + d\sigma_{cp} + eT}, \quad R^2 = 0.6, \quad RMSE = 0.003 \quad (16)$$

When ET is the adobe's elastic toughness, σ_{cp} is the maximum stress, T is the calculated toughness, $a = 0.002$, $b = 0.0006$, $c = -0.02$, $d = -0.08$, $e = -3.8$,

Calculating adobes' stress corresponding to maximum elastic modulus (σ_{c0}) :

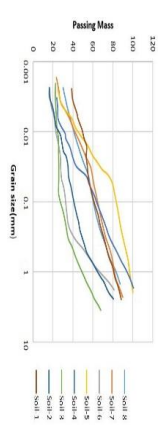
$$\sigma_{c0} = \frac{\sigma_{cp} ET}{a + b\sigma_{cp} + cET}, \quad R^2 = 0.8, \quad RMSE = 0.2 \quad (17)$$

When σ_{c0} is the adobe's stress corresponding to maximum elastic modulus, ET is the calculated elastic toughness, σ_{cp} is the peak stress, $a = -0.0004$, $b = 0.0008$, $c = 1.5$

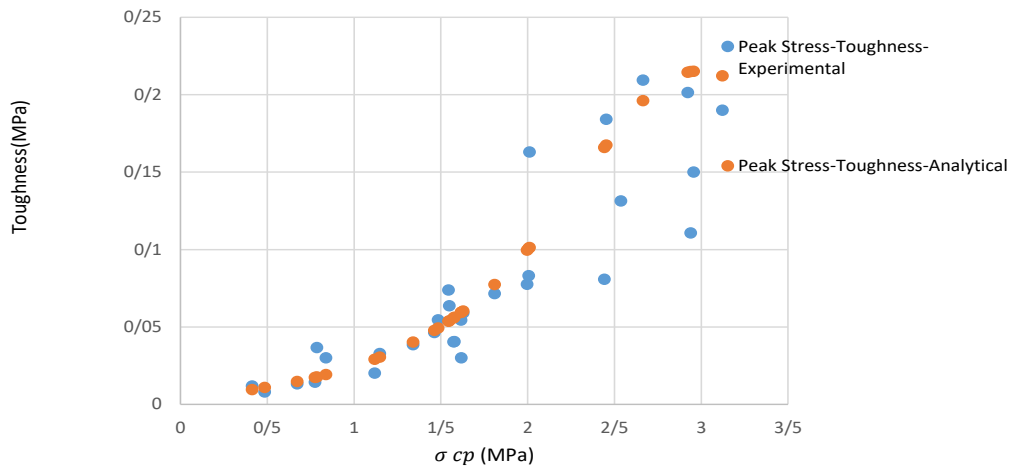
Calculating adobes' strain corresponding to maximum elastic modulus (ϵ_{0c}) :

$$E_{0c} = \frac{\sigma_{c0}}{E_{0c}} \quad (18)$$

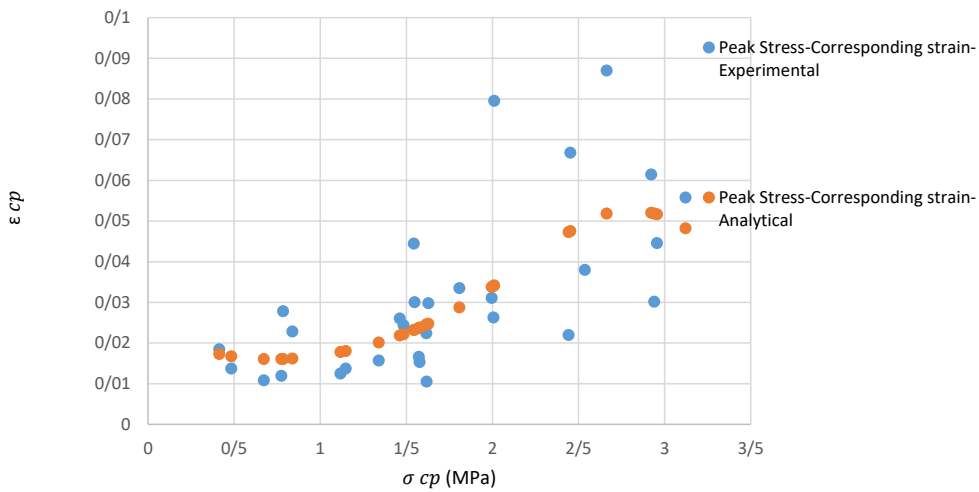
Table 5. Adobe specimens' characteristics in different studies

Reference	Adobes Making Procedure	Grain size distribution	Reinforcing fibers%	Tested specimen dimensions	Rate of loading	σ_{cp} (MPa)	ϵ_{cp}	σ_{c0} (MPa)	ϵ_{c0}	E_{0c} (MPa)	ϵ_{cu}	Toughness (MPa)	Elastic Toughness (MPa)		
[27]	By mixing machine soil, water and straw fibers mixed with each other, then prismatic wood formworks were filled with the mixture which was pressed by	Silt+ Clay<0.075mm	3%	4.75<Gravel<75mm	Cubic specimens with 70mm edges	Displacement-control uniaxial tests at a displacement rate of 0.01mm/s	1.12	0.013	0.53	0.003	194	0.023	0.02	0.0007	
							0.48	0.014	0.24	0.004	66	0.021	0.008	0.0004	
							0.67	0.011	0.29	0.002	138	0.024	0.013	0.0003	
							0.77	0.012	0.32	0.003	125	0.023	0.014	0.0004	
							1.48	0.024	0.24	0.001	289	0.046	0.05	0.0001	
							1.57	0.015	1.32	0.01	130	0.034	0.041	0.0006	
							2	0.026	0.63	0.004	161	0.051	0.083	0.001	
							1.34	0.016	0.58	0.003	167	0.034	0.039	0.0008	
							1.62	0.011	0.99	0.004	286	0.023	0.03	0.0014	
							1.57	0.017	1.18	0.009	133	0.034	0.04	0.0042	
0.41	0.019	0.17	0.003	51	0.034	0.012	0.0003								
This study	they were made by cutting the adobe ingots produced using a spiral	Silt+ Clay<0.075mm	85.6%	4.75<Gravel<75mm	Cubic specimens with 100mm edges	Displacement-control uniaxial tests at a displacement rate of 0.01mm/s	1.81	0.034	1.36	0.016	87	0.052	0.071	0.0103	
							1.54	0.044	1.09	0.024	45	0.064	0.074	0.0129	
							1.46	0.026	0.83	0.012	71	0.046	0.046	0.0036	
							2.94	0.03	1.46	0.008	182	0.05	0.11	0.0054	
[3]	They were made by adding 15% water to 8 different soil type existing adobes, kneading, fitting and pressing them in a		No added fibers	Cubic specimens with 50mm edges	Displacement-control uniaxial tests	0.79	0.028	0.6	0.018	33	0.058	0.037	0.0054		
						0.84	0.023	0.43	0.005	93	0.044	0.03	0.001		
						1.15	0.014	0.49	0.003	144	0.034	0.033	0.0007		
						1.63	0.03	0.41	0.003	147	0.047	0.059	0.0006		
						1.55	0.03	0.89	0.009	98	0.05	0.064	0.0037		
						1.62	0.022	0.67	0.003	196	0.041	0.054	0.001		
						1.9	0.03	1.17	0.011	111	0.051	0.078	0.006		
						2.44	0.022	1.7	0.008	220	0.04	0.081	0.0071		
[28]	The mixtures were made by mixing	Silt+ Clay	90%	Gravel	Not equal cubic specimens: 150*230*130 mm ³	Both Displacement and force control uniaxial tests at the	2.96	0.045	1.64	0.009	173	0.061	0.15	0.007	

The mixtures were made by mixing machine, then they were compacted in wooden moulds in separate layers	Silt+ Clay	Gravel	No added fibres	Not equal cubic specimens: 150*230*130 mm ³ Load direction was parallel to the shorter edge	Both Displacement and force control uniaxial tests at the rate of 0.03 N/mm ² s	2.96	0.045	1.64	0.009	173	0.061	0.15	0.007			
			No added fibres			3.12	0.056	2.08	0.018	118	0.076	0.19	0.018			
			No added fibres			2.01	0.08	0.68	0.009	79	0.1	0.16	0.0027			
		Coarse sand and Straw fibres: mean percentage by volume for each one: 0.5%	2.45			0.067	0.65	0.004	151	0.089	0.18	0.0012				
			2.9			0.06	1.1	0.008	142	0.083	0.2	0.0049				
			6%			14.8%	79%	6%	14.8%	79%	6%	14.8%	79%			
	Silt+ Clay	Sand	Gravel			Straw fibers, length lower than 25mm- mean percentage by volume: 40%	Cubic specimen with 50mm edges	Displacement-control: 0.1 mm/s	2.66	0.087	1.38	0.032	44	0.11	0.21	0.0176
									2.66	0.087	1.38	0.032	44	0.11	0.21	0.0176
									2.66	0.087	1.38	0.032	44	0.11	0.21	0.0176
		2.66							0.087	1.38	0.032	44	0.11	0.21	0.0176	
		2.66							0.087	1.38	0.032	44	0.11	0.21	0.0176	
		2.66							0.087	1.38	0.032	44	0.11	0.21	0.0176	
Silt+ Clay	Sand	Gravel	Straw fibers, length lower than 25mm- mean percentage by volume: 40%	Cubic specimen with 50mm edges	Displacement-control: 0.1 mm/s	2.66	0.087	1.38	0.032	44	0.11	0.21	0.0176			
						2.66	0.087	1.38	0.032	44	0.11	0.21	0.0176			
						2.66	0.087	1.38	0.032	44	0.11	0.21	0.0176			
	2.66					0.087	1.38	0.032	44	0.11	0.21	0.0176				
	2.66					0.087	1.38	0.032	44	0.11	0.21	0.0176				
	2.66					0.087	1.38	0.032	44	0.11	0.21	0.0176				
Silt+ Clay	Sand	Gravel	Straw fibers, length lower than 25mm- mean percentage by volume: 40%	Cubic specimen with 50mm edges	Displacement-control: 0.1 mm/s	2.66	0.087	1.38	0.032	44	0.11	0.21	0.0176			
						2.66	0.087	1.38	0.032	44	0.11	0.21	0.0176			
						2.66	0.087	1.38	0.032	44	0.11	0.21	0.0176			
	2.66					0.087	1.38	0.032	44	0.11	0.21	0.0176				
	2.66					0.087	1.38	0.032	44	0.11	0.21	0.0176				
	2.66					0.087	1.38	0.032	44	0.11	0.21	0.0176				



(a)



(b)

Fig. 10. Comparison between experimental data and calculated ones for adobes' toughness (a), and strain corresponding to peak stress versus the peak stress (b)

When E_{0c} is the calculated maximum elastic modulus and σ_{c0} is the calculated stress corresponding to maximum elastic modulus,

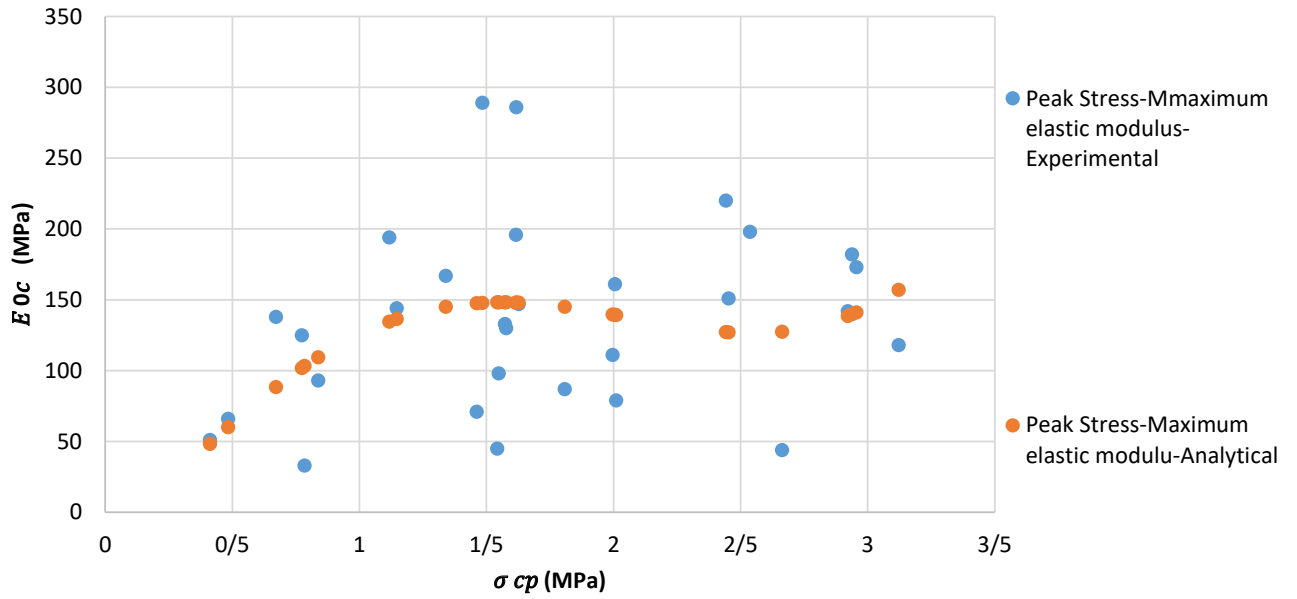
Calculating adobes' ultimate strain (ϵ_{cu})

$$\epsilon_{cu} = \dots, R^2 = 0.9,$$

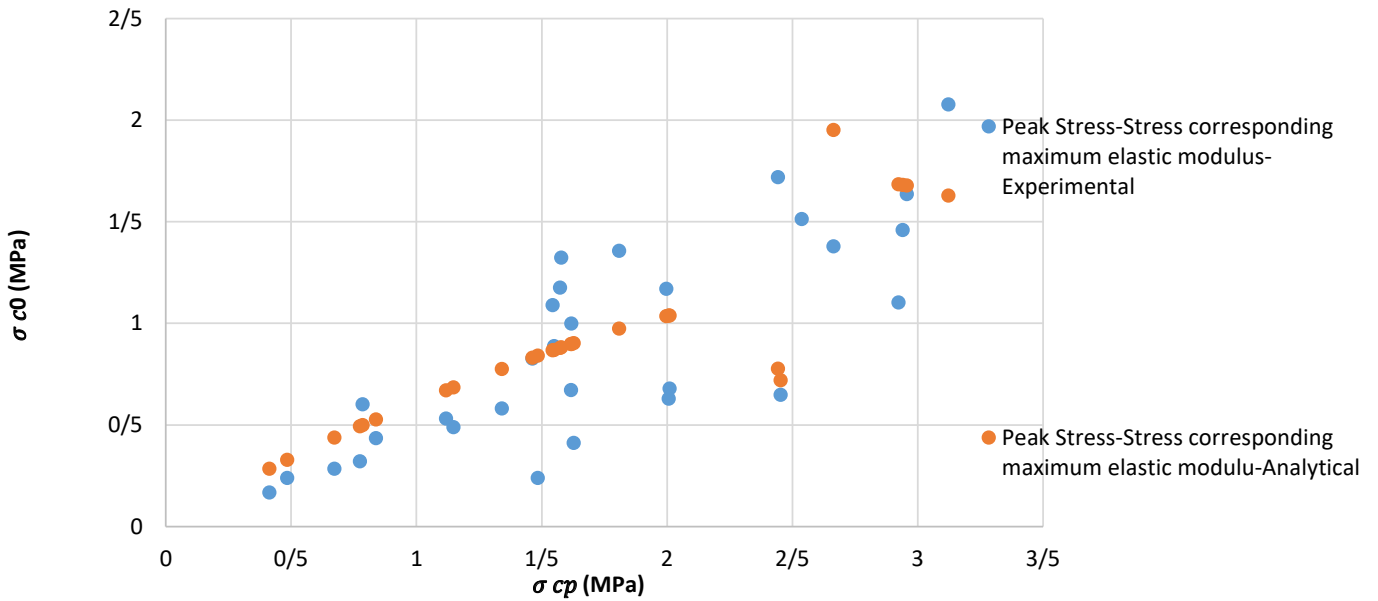
RMSE=0.006

When σ_{cp} is the peak stress, ϵ_{cp} is the calculated strain corresponding to the peak stress, $a = -0.005$, $b = 0.02$, $c = 2$, $d = 0.3$, $e = 3$,

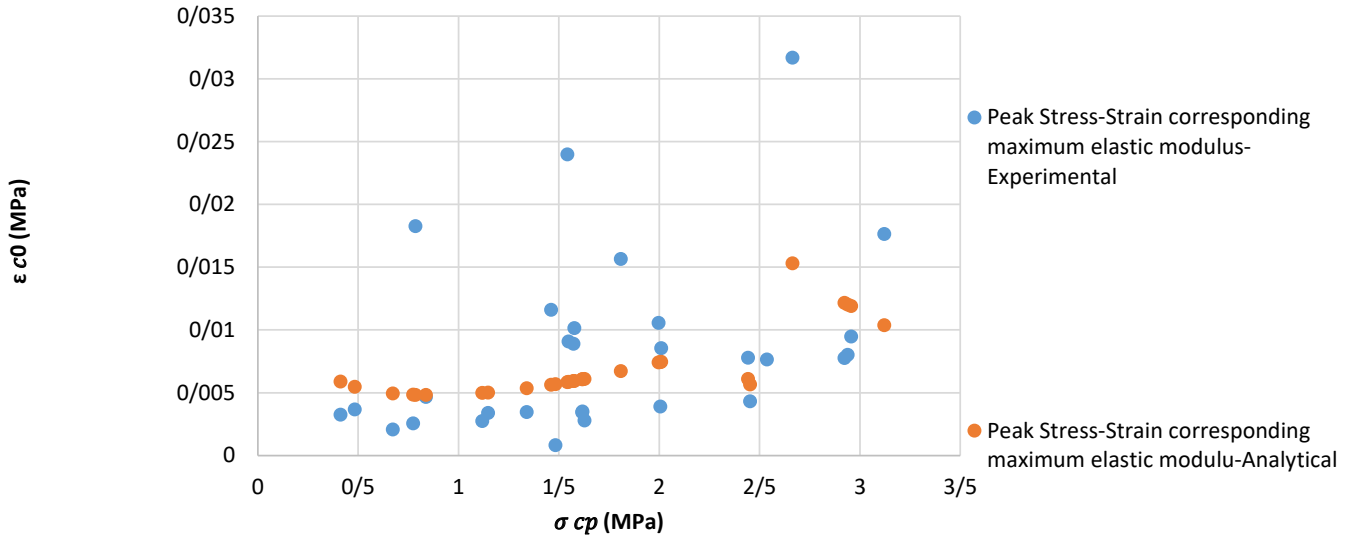
the comparison between experimental data and calculated ones for adobes' maximum elastic modulus, stress corresponding to maximum elastic modulus, its corresponding strain, and the ultimate strain versus the peak stress are presented in Fig.11.



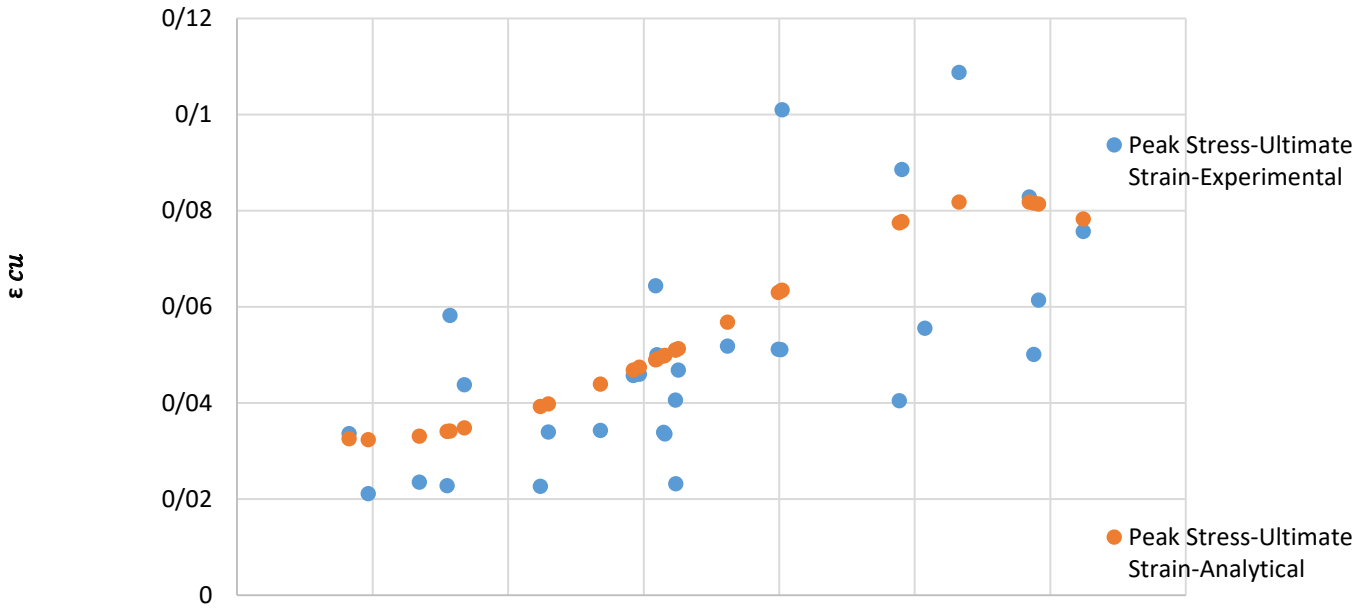
(a)



(b)



(c)



(d)

Fig. 11. Comparison between experimental data and calculated ones for adobes' maximum elastic modulus (a), stress corresponding to maximum elastic modulus (b), its corresponding strain (c) and the ultimate strain (d) versus the peak stress

6- A mathematical model for predicting the compressive stress-strain curve

According to estimating the elastic part of the compressive stress-strain curve of adobes by assessing E_{0c} and σ_{c0} using proposed equations, it is trying to suggest a stress-strain relationship for the inelastic part of different adobes by comparing normalized inelastic behaviors of different studied adobe specimens by determining σ_{cp} and ε_{cp} . Since the amount of compressive stress and corresponding strain are different in every case, it is decided to give normalized quantities for plotting of stress-strain curves in order to be comparable. For doing this normalization, in each case, the uniaxial compressive stresses were divided over the peak stress, σ_{cp} , and similarly, the axial strains were divided over compressive strain at the instant of peak stress, ε_{cp} . The results in terms of uniaxial compressive stress and strain for those cases reported in table 5 are plotted in figure 12 and the normalized quantities for the similar data are plotted in fig. 13

using the software of Plot Digitizer-Version 2.0.

According to Fig.13, it is shown that all the specimens show an increasing elastic modulus up to the maximum one due to progressive densification. By starting the inelastic behavior, the elastic modulus decreases gradually to zero at peak stress point and in the descending part become negative. By assumed E_0 to be the maximum of Young modulus, the schematic complete normalized compressive stress-strain curves for all different kinds of adobes can be presented in Fig.14. The normalized inelastic parts of them are illustrated in Figure 15 as well.

It is stated by Fig.14 and 15 that inelastic parts of compressive stress-strain relationships have the same general shape which does not begin from zero. This leads to consider the Hoerl model to predict the inelastic part of the compressive stress-strain curve. The curve formulation can be presented as follow.

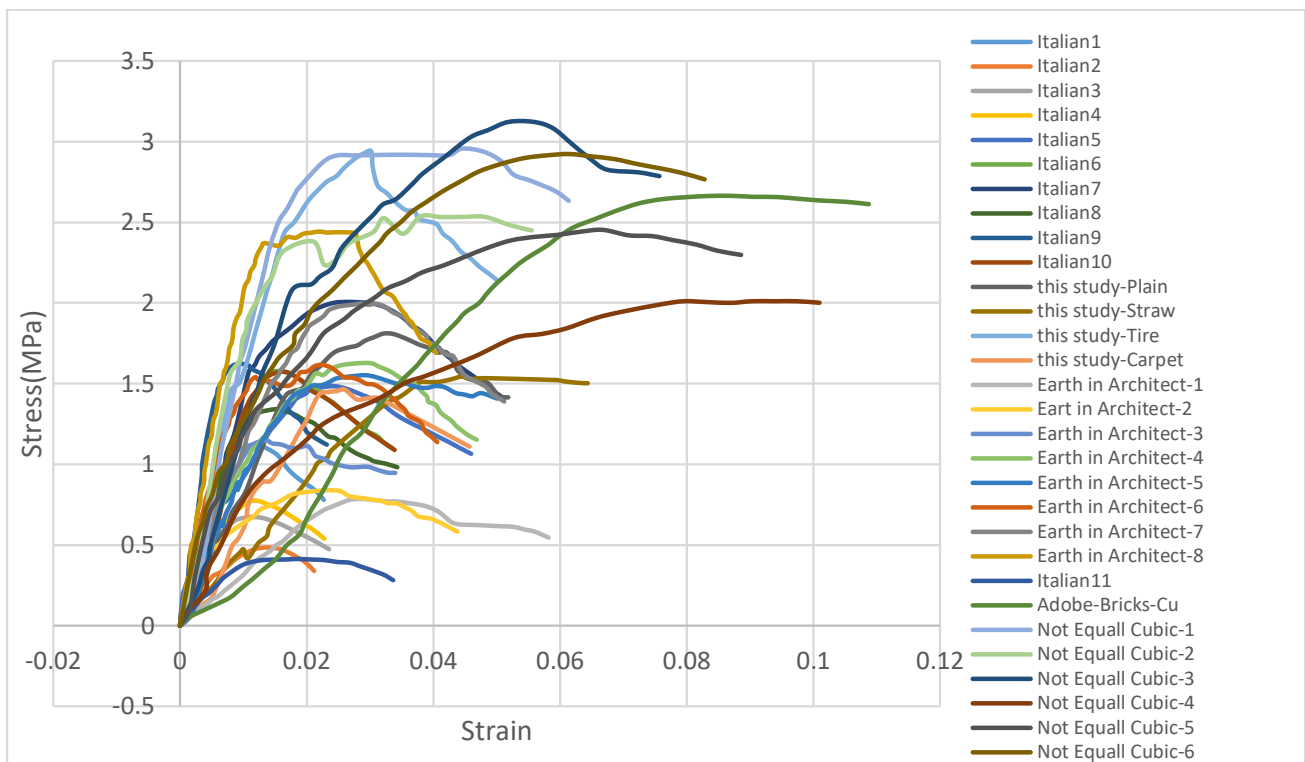


Fig. 12. Uniaxial compressive stress-strain curves for investigated specimens

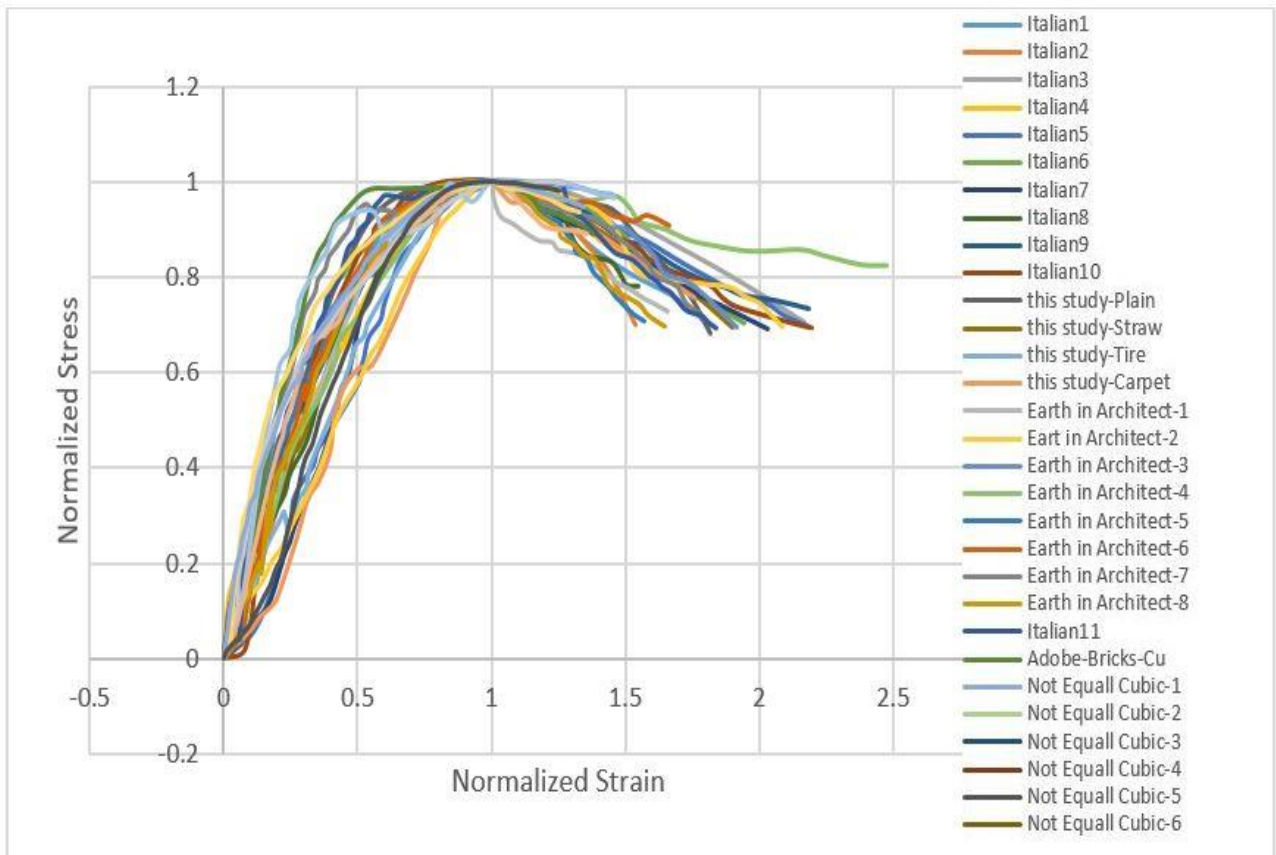


Fig. 13. Normalized uniaxial compressive stress-strain curves for investigated specimens

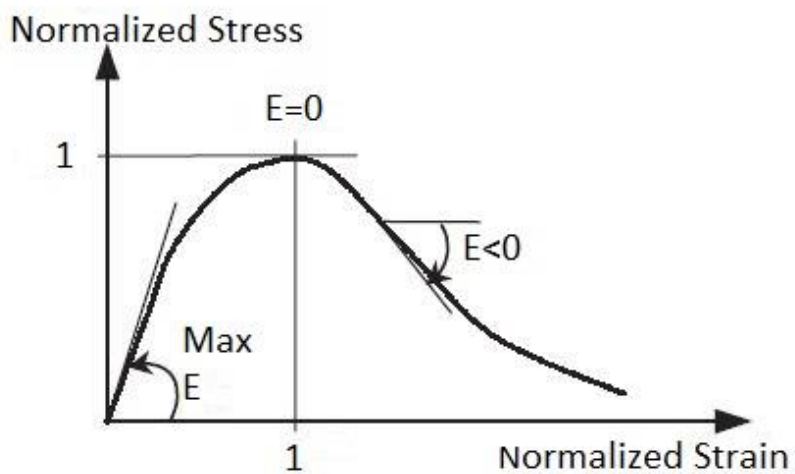


Fig. 14. Schematic normalized uniaxial compressive stress-strain curves for different adobe specimens

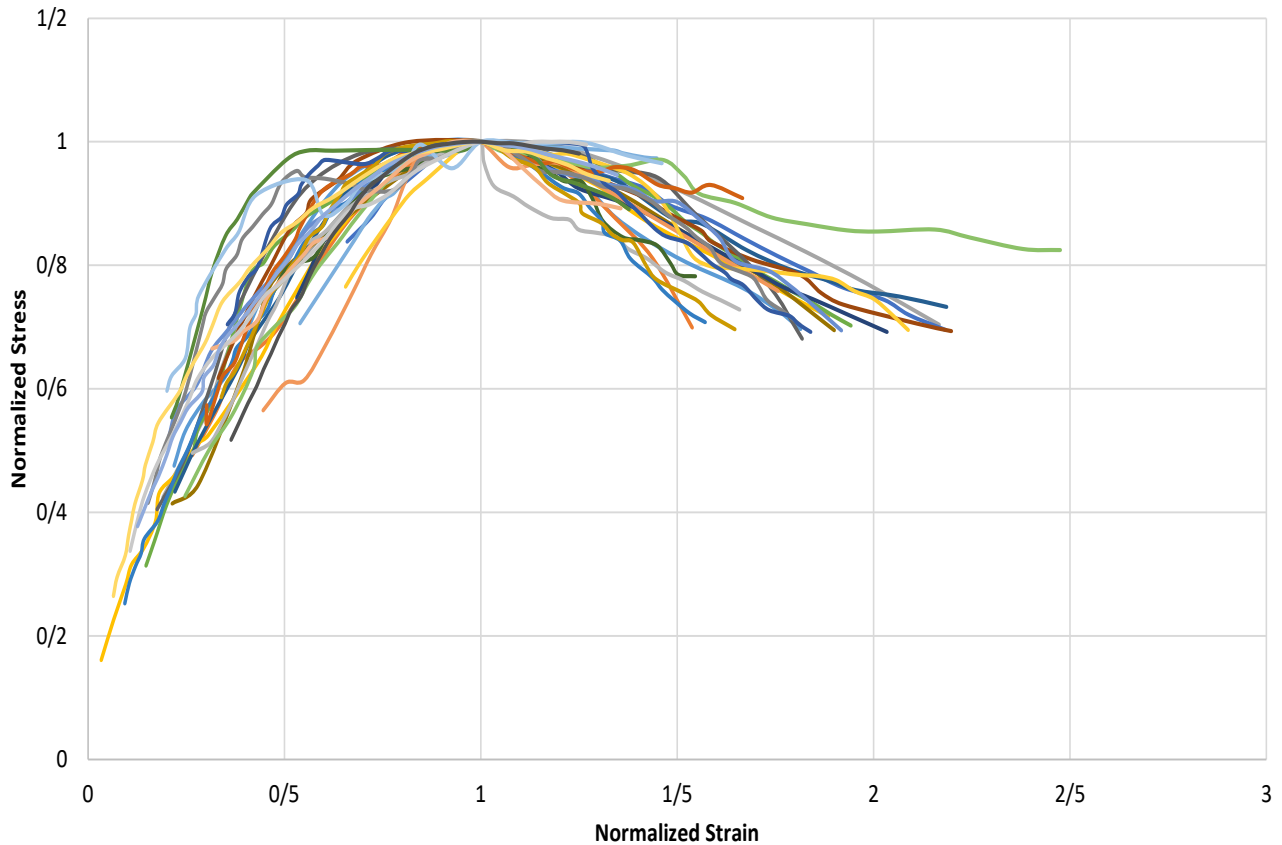


Fig. 15. Normalized inelastic parts of uniaxial compressive stress-strain curves for investigated specimens

A mathematical model for predicting the inelastic part of the compressive stress-strain curve

$$\sigma_c = AB^{\epsilon_c} \epsilon_c^C \tag{20}$$

When σ_c is the normalized inelastic stress and ϵ_c is the normalized corresponding strain. Parameters of A, B and C indicate the effects of different compositions, compacting types, curing conditions, and testing condition. In order to evaluate these parameters for the range of studied data in table 5, a regression analysis was performed using the software CurveExpert Professional 1.6.5.

Calculating the parameter of ‘B’

$$B = a + bT + c(T - ET) + dT^2 + e(T - ET)^2 + fT^3 + g(T - ET)^3 + h * T * (T - ET) + i * T^2 * (T - ET) + j * T * (T - ET)^2, \tag{21}$$

$R^2 = 0.6$, RMSE= 0.09

When T is the calculated toughness, ET is the calculated elastic toughness, a= 0.3, b= 30, c= -32, d= -1e4, e= -1e4, f= 1e6, g= -1e6, h=2e4, i= -2e6, j=3e6.

Calculating the parameter of ‘A’:

$$A = ab^{\frac{1}{B}} B^c \quad , \quad R^2 = 0.95 \quad , \quad RMSE= 0.3 \tag{22}$$

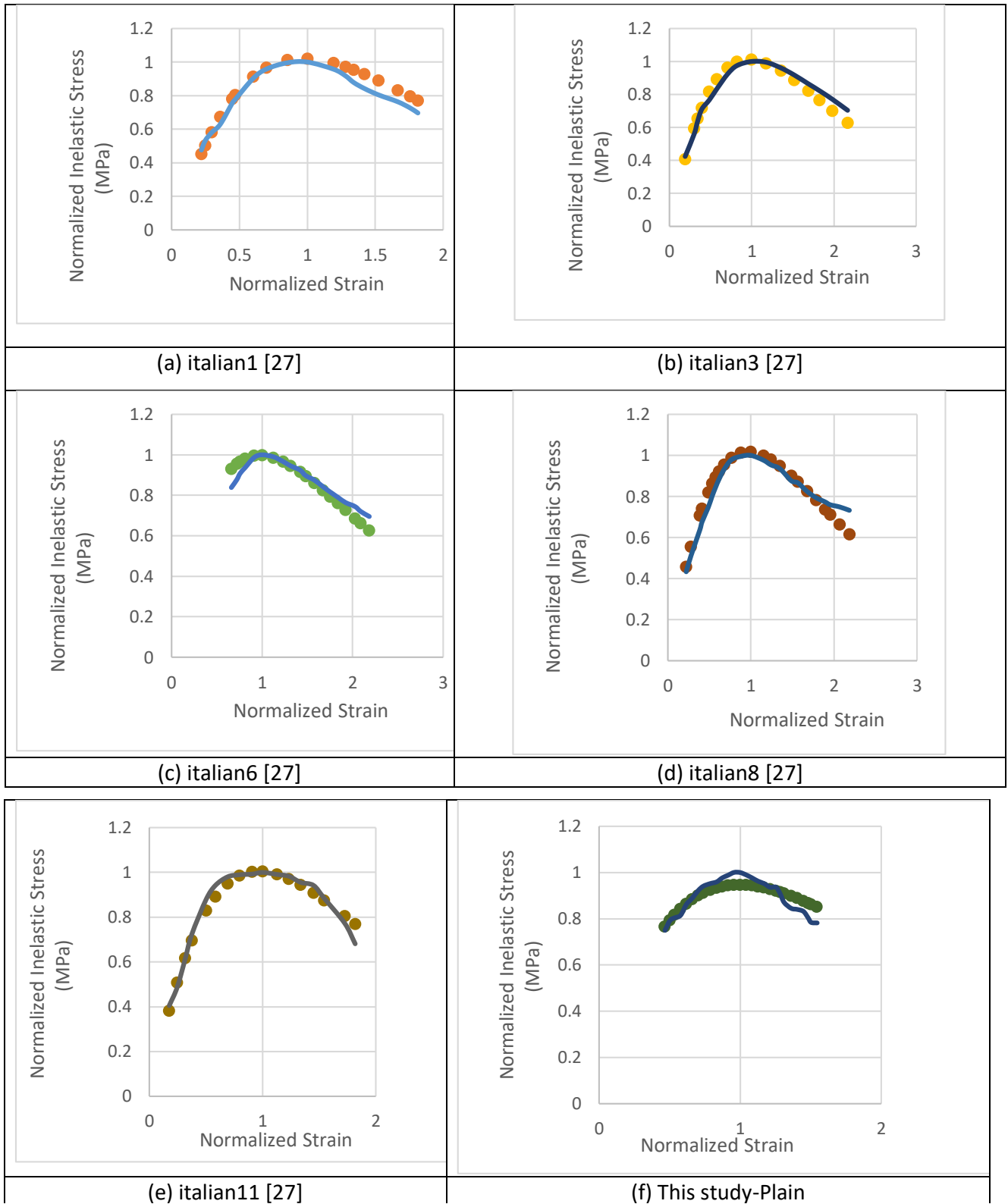
When B was calculated in the last step, a= 0.67, b= 0.8, c= -1.97.

Calculating the parameter of ‘C’:

$$C = ab^{\frac{1}{B}} B^c \quad , \quad R^2 = 0.95 \quad , \quad RMSE= 0.1 \tag{23}$$

When B was calculated previously, a= 0.43, b= 0.96 c=-0.94

The following diagrams in Fig.16 present the comparison between experimental data and calculated ones for normalized inelastic part of compressive stress-strain curves for 10 studied specimens.



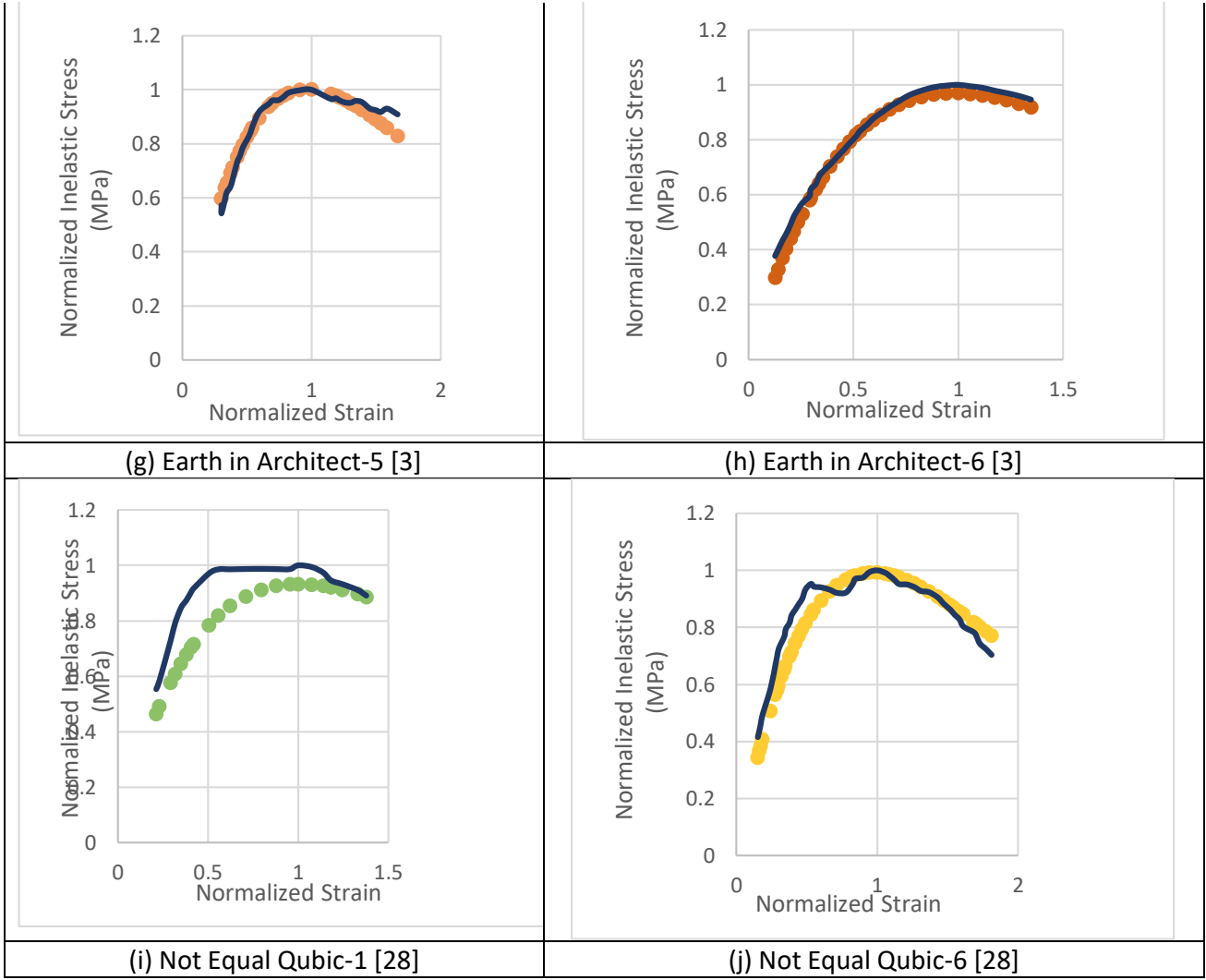


Fig. 16. A comparison between the predicted normalized inelastic parts of uniaxial compressive stress-strain curves by suggested model and experimental results; dash ones are analytical and smooth ones are experimental results. The reference numbers are under each figure, their names are according to figures 12, 13.

Fig.16 illustrates that predicted curves fit the experimental ones so well. So it seems that the suggested formulations are successful in predicting the complete stress-strain relationship for different adobes specimens with different composition, compacting type, curing condition, and testing condition with a very good agreement.

There are some researchers who investigated the uniaxial compressive behavior of different kinds of adobes. Fig17 presents a comparison of proposed model predictions with other models for some experimental results. It is important to mention that all these models need to determine both maximum compressive stress and its corresponding strain experimentally and also they do not pay attention to the required parameters for an adequate simulation by software while the proposed model by authors needs to determine only maximum compressive stress experimentally and it pays attention to the required parameters for the software simulation. The formulation of the model 1 and 2 in Figure 17 are as follow.

$$\begin{cases} 1.44065\bar{\varepsilon}_c + 0.11869\bar{\varepsilon}_c^2 - 0.55935\bar{\varepsilon}_c^3 \\ 1.26585 - 0.28512\bar{\varepsilon}_c + 0.02752\bar{\varepsilon}_c^2 - 0.00009\bar{\varepsilon}_c^3 \end{cases} \quad (1)$$

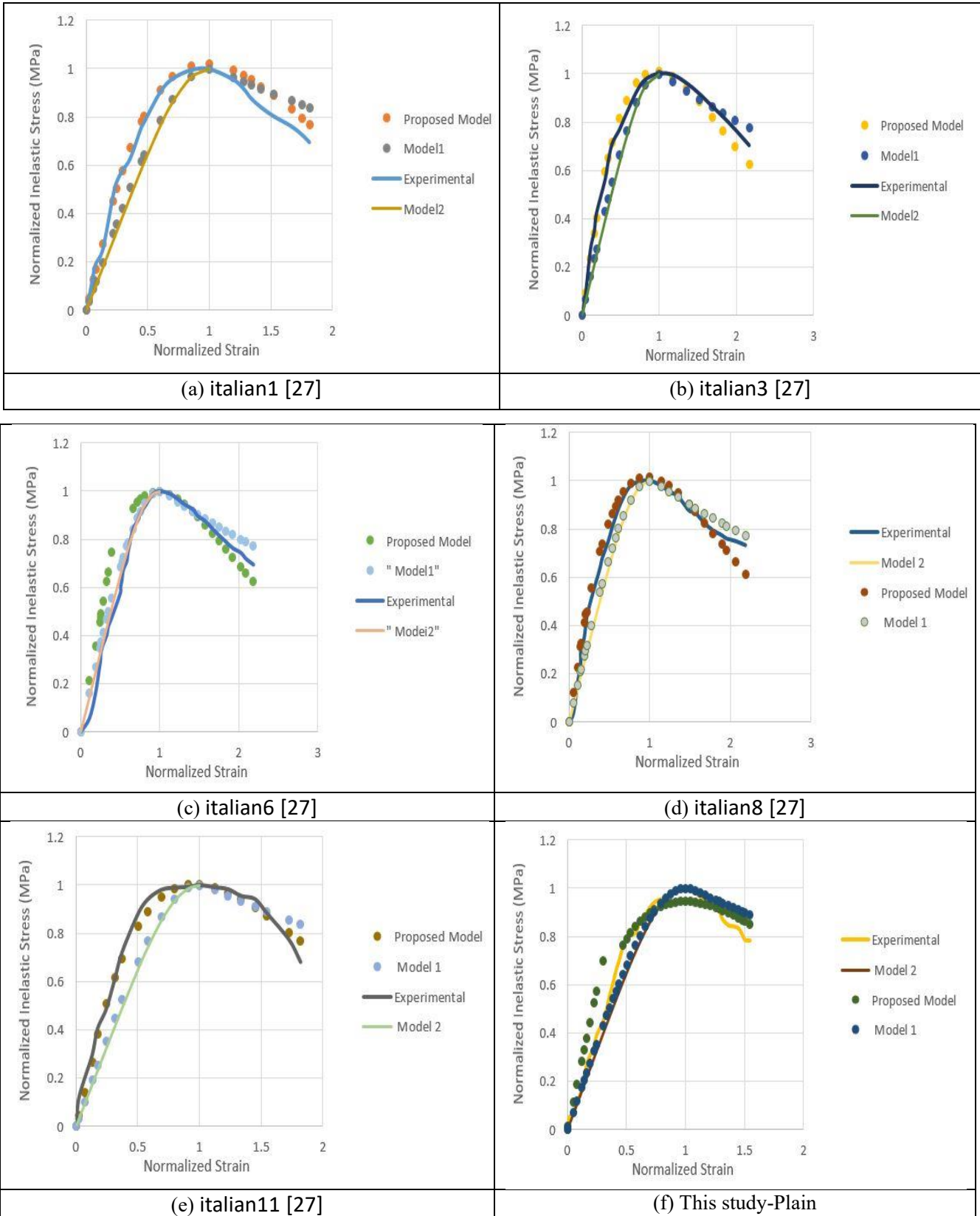
When $\bar{\sigma}_c = \frac{\sigma_c}{f_b}$ and $\bar{\varepsilon}_c = \frac{\varepsilon_c}{\varepsilon_{fb}}$. this formulation was

adopted by solving an optimizing problem for maximizing the coefficient of determination (R^2) for a stress-strain curve which has the best fit with experimental results [11].

The second formulation is only for pre-peak behavior [5]

$$\bar{\sigma}_c = \frac{4.11\bar{\varepsilon}_c}{4.11 - 1 + (\bar{\varepsilon}_c^{4.11})} \quad (25)$$

this formulation was adopted by solving an optimizing problem too.



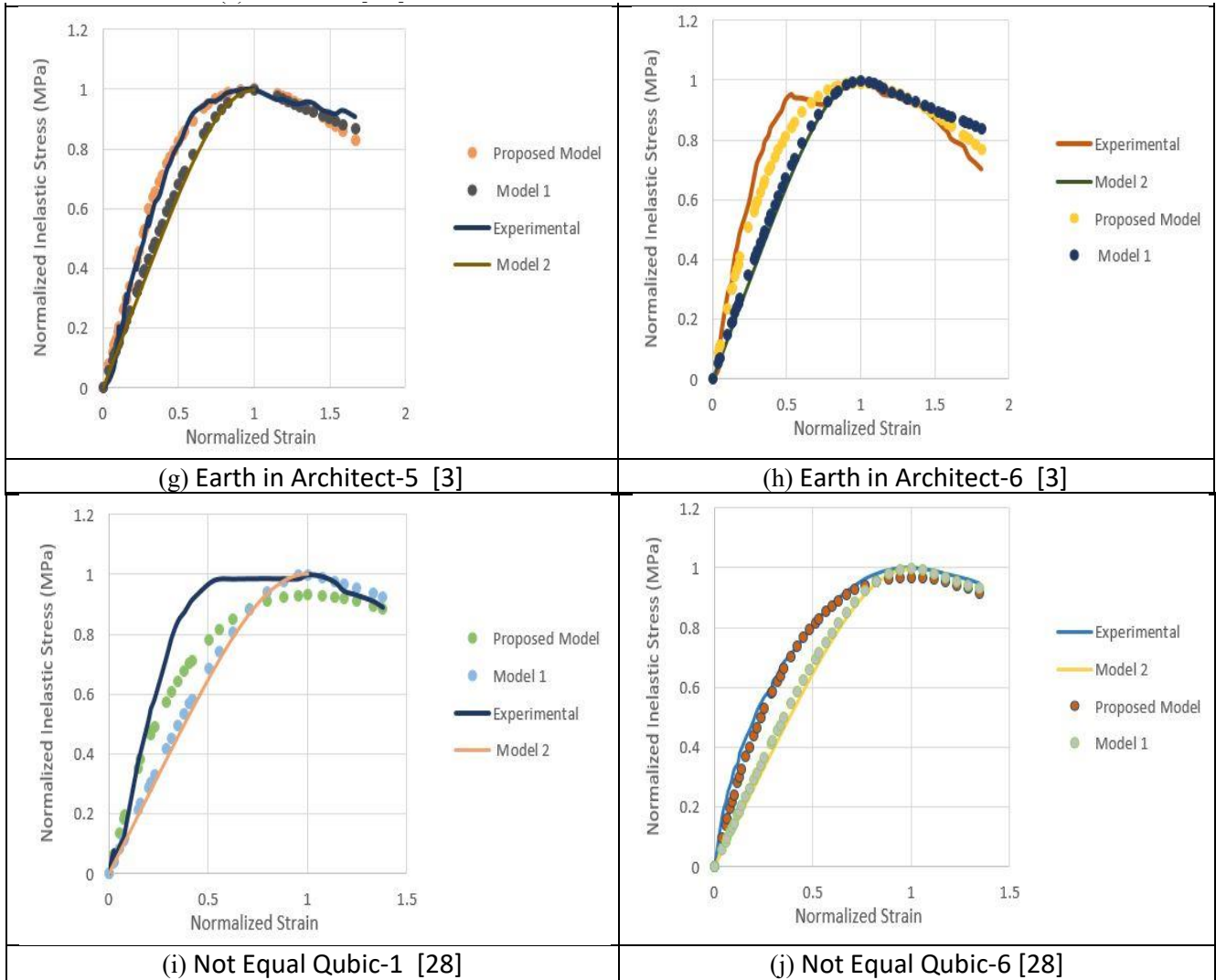


Fig. 17. A comparison of proposed model with other works for some compressive experimental results. The reference numbers are under each figure, their names are according to figures 12, 13.

As it is illustrated in Fig.17, the current model is to some extent more successful in predicting both linear and nonlinear behavior of different adobes and the required parameters for simulating adequately by software. To have a more detailed collation, Table 6 presents a comparison between the toughness of different models that predicted compressive stress-strain curves, according to Fig.17, with the experimental results.

7- Conclusions

The current study is divided into three separate sections: an experimental study, numerical simulation, and developing mathematical relations to predict different plain or short fibers reinforced adobes' compressive stress-strain behavior which is suitable for further numerical analysis and introduction to the ABAQUS software. They are explained briefly as follows:

- In this study, it is tried to present a model for predicting

the relationship between uniaxial compressive stress and corresponding strain which can simulate the structural behavior of plain and short fiber reinforced adobes with concrete damage plasticity model in ABAQUS.

- Initially, it was attempted to illustrate experimentally the compressive properties of four different plain and short fiber reinforced adobes
- In order to determine desired mechanical parameters for presenting an appropriate compressive stress-strain curve, it was tried to present material models for each mix design and simulate compressive behavior of them with concrete damage plasticity in ABAQUS. By verifying the numerical results with experimental ones, the essential parameters were defined.
- After determining the essential parameters, the proposed equations were presented for calculating the parameters (equations numbers 13-19) when the only needed

Table 6. Comparing toughness of different assumed models for predicting of compressive stress- strain curves with experimental results.

specimen	Experimental	Model 1	Model 2	Proposed Model
(a) Italian1	1.4	1.3	0.8	1.46
%comparing with experimental results	-	-7.14286	-42.8571	4.285714286
(b) Italian3	1.7	1.6	1	1.7
%comparing with experimental results	-	-5.88235	-41.1765	0
(c) Italian6	1.5	1.6	0.8	1.45
%comparing with experimental results	-	6.666667	-46.6667	-3.333333333
(d) Italian8	1.7	1.7	1	1.7
%comparing with experimental results	-	0	-41.1765	0
(e)Italian11	1.47	1.37	1	1.45
%comparing with experimental results	-	-6.80272	-31.9728	-1.360544218
(f) Current study- Plain	1.1	0.5	0.6	0.9
%comparing with experimental results	-	-54.5455	-45.4545	-18.18181818
(g)Earth in arch5	1.33	1.2	0.7	1.33
%comparing with experimental results	-	-9.77444	-47.3684	0
(h)Earth in arch6	1.47	1.36	1	1.44
%comparing with experimental results	-	-7.48299	-31.9728	-2.040816327
(i)not equal1	1.1	0.9	0.6	1
%comparing with experimental results	-	-18.1818	-45.4545	-9.090909091
(j)not equal6	1.06	0.95	0.6	1.03
%comparing with experimental results	-	-10.3774	-43.3962	-2.830188679

experimentally determined parameter was maximum compressive stress which can be obtained easily.

- In the end a mathematical model was developed for predicting of the complete stress-strain curve in both ascending and descending branches (equations numbers 20-23), for plain and short fibers reinforced adobes with different compositions, compacting, curing, and testing condition according to the current study and literature.
- The following conclusions can be remarked:
 - Concrete damage plasticity is a suitable constitutive material model for modeling plain or fibers reinforced adobes in ABAQUS software.
 - Adobes are able to be predicted correctly by the suggested FE model when the main required mechanical properties include, σ_{Cp} , ε_{Cp} , σ_{C0} , ε_{C0} , E_{0c} where σ_{Cp} is the peak compressive strength, ε_{Cp} is the axial strain at peak compressive strength. σ_{C0} and ε_{C0} are the compressive strength and it's a corresponding strain at the point with maximum Yong's modulus and E_{0c} is the maximum compressive Young's modulus.
 - The proposed formulations are able to predict, σ_{cp} , ε_{cp} , σ_{c0} , ε_{c0} , E_{0c} and ε_{cu} when ε_{cu} is the ultimate strain.
 - The suggested model is compatible with the behavior of different adobes with different compositions, compacting, curing, and testing condition.
 - The suggested model and formulations are to some extent more successful in predicting the linear and nonlinear behavior of different adobes according to other models.
 - The only needed experimentally determined parameter for the proposed model is σ_{Cp} .

Compliance with Ethical Standards:

The authors declare that they have no conflict of interest.

References

- [1] D. Silveira, H. Varum, A. Costa. Influence of the testing procedures in the mechanical characterization of adobe bricks. *Construction and Building Materials*, vol. 40. Pp. 719- 728. 2013.
- [2] M.S. Islam, K. Iwashita. Earthquake resistance of adobe reinforced by low cost traditional materials. *Journal of Natural Disaster Science*, vol. 32, no.1, pp.1-21. 2010.
- [3] F. Fratini, E. Pecchioni, L. Roverto, U. Tonietti. The earth in the achitecture of the historical center of Lamezia Temrme (Italy): Characterization for restoration., *Applied Clay Science*, vol. 53, no. 3, pp. 509-516. 2011.
- [4] N. Augenti, F. Parisi. Constitutive models for tuff masonry under uniaxial compression. *Journal of Materials in Civil Engineering*, vol. 22, no. 11, pp. 1102-1111. 2010.
- [5] E. Adorni, E. Coisson, D. Ferretti. In situ characterization of archaeological adobe bricks. *Construction and Building Materials*, vol. 40, pp. 1-9. 2013.
- [6] Zdenek P. Bazant. Concrete fracture models: testing and practice. *Engineering Fracture Mechanics* 69, 165-205. 2002.
- [7] S.S. Ali, A.W. Page. Finite element model for masonry subjected to concentrated Loads. *Journal of Structural Engineering*, vol. 114. 1987.
- [8] S.K. Arya, G.A. Hegemier. On nonlinear response prediction of concrete masonry assemblies. *North American Masonry Conference*, Boulder, Colorado, USA, pp.19.1-19.24. 1987.
- [9] H.R. Lotfi, Shing. Interface model applied to fracture of masonry structures. *ASCE*, Vol.120, No.1, pp.63-80. 1994.
- [10] Domingo, J. Carreira, Kuang-Han Chu. Stress-strain relationship for plain concrete in compression. *ACI Journal*. 1985.
- [11] R. Illampas, Experimental and computational investigation of the structural response of adobe structures, Phd thesis, university of Cyprus, 2013.
- [12] ASTM D 2487-98. "Standard practice for classification of soils for engineering purposes (unified soil classification system)". West Conshohocken: ASTM International; 2017.
- [13] ASTM D 4318- 98. "Standard Test Methods for Liquid Limit, Plastic Limit, and Plasticity Index of Soils". West Conshohocken: ASTM International; 2017.
- [14] M. Abbaspour, F. Moghadas Nejad. Reuse of waste tire textile fibers as soil reinforcement. *Journal of Cleaner Production*, pp. 1059,1071
- [15] CEN- "Eurocode 6: Design of masonry structures". ENV 1996-1-1:1995, CEN, Brussels, Belgium, 1995.
- [16] E.E.Gdoutos, *Fracture Mechanics an Introduction*, second edition, Springer, 2005.
- [17] EN 1998. "Eurocode 8: Design of structures for earthquake resistance". Brussels; 2004 (Part 1) and 2005 (Part3).
- [18] F. Faghii-khorasani, M.Z. Kabir, K.Ghavami, M. Ahmadi. Predicting of compressive stress-strain curves of structural adobe cubes Based on Acoustic Emission (AE) Hits and Weibull Distribution. *International Journal of structural integriyu*. 2019.
- [19] Mark F. Carlos. Acoustic Emission: Heeding the Warning Sounds from Materials. https://www.astm.org/SNEWS/OCTOBER_2003/carlos_oct03.html.
- [20] Jun Zhou, A study of acoustic emission technique for concrete damage detection, Maser thesis, Michigan Technological University, 2011
- [21] ASTM C469/C469M–10 Standard test method for static modulus of elasticity and Poisson's ratio of concrete in compression. West Conshohocken: ASTM International; 2010.
- [22] F.Frantini, E.Pecchioni,L.Rovero,U.Tonietti. The earth in the architecture of the historical centre of Lamezia Terme (Italy): Characterization for restoration. *Applied Clay Science*, issue 3, Elsevier, 2011.
- [23] J. Lubliner, J. Oliver, S. Oller, E. Onate. A Plastic-damage model for concrete. *International Journal of Solid and Structures*, vol. 25, no.3, pp. 299-326. 1989.
- [24] J. Lee, G. Fenves. Plastic- damage model for cyclic loading of concrete structures. *Journal of Engineering Mechanics*, vol. 124. No. 8, pp. 892-900. 1988.

- [25] B.L. Wahlanthri, et.al, A material model for flexural crack simulation in reinforced concrete element using ABAQUS, First International Conference on Engineering, Designing and Developing the Built Environment for Sustainable Wellbeing, Queensland University of Technology, Queensland University of Technology, Brisbane, Qld, pp. 260-264.
- [26] F. Faghihkhorsani, M.Z. Kabir ,M.A. Rastaak, Tensile characterization of composite adobe specimens reinforced with short fibers, an experimental study, 2018, The Biennial International Conference on Experimental Solid Mechanics, Tehran.
- [27] F.Parisi, D.Asprone, L.Fenu, A.Prota. Experimental characterization of Italian composite adobe bricks reinforced with straw fibers. *Composite Structure* 122, 300-307, 2015.
- [28] E.Quagliarini, S.Lenci. The influence of natural stabilizers and natural fibres on the mechanical properties of ancient Roman adobe bricks. *Journal of Cultural Heritage* 11, 309-314, 2010.
- [29] R.Illampas, I.Ioannou, D.C.Charpis. Adobe bricks under compression: Experimental investigation and derivation of stress–strain equation. *Journal of Construction and Building Materials* 53, 83-90, 2014.

Appendix(A)

Table A. Compressive Stress-Strain Values

Stress(σ_c)(MPa)	Plain, $E_c=87\text{MPa}$		Reinforced by Tire fibers, $E_c=183\text{MPa}$		
	Inelastic Strain (ϵ_c^{in})	Damage (d_c)	Stress(σ_c)(MPa)	Inelastic Strain (ϵ_c^{in})	Damage (d_c)
1.356555546	0	0	1.45893288	0	0
1.433014568	0.00124959	0	1.50493789	0.001391125	0
1.455045134	0.002385593	0	1.58852444	0.002212061	0
1.474051896	0.003774909	0	1.6905778	0.003030973	0
1.55893437	0.005149101	0	1.75699348	0.003498035	0
1.609043108	0.006566631	0	1.84252391	0.004081588	0
1.668439241	0.007983144	0	1.98539861	0.005133196	0
1.701917061	0.009165327	0	2.08745196	0.00585724	0
1.722435726	0.01082327	0	2.16391098	0.006512938	0
1.735934847	0.012363398	0	2.25484106	0.007119616	0
1.766712843	0.013664462	0	2.33885959	0.007727051	0
1.788311437	0.015085117	0	2.44099394	0.00858153	0
1.809910031	0.016505771	0	2.4999851	0.01005738	0
1.808830101	0.017928912	0	2.57434598	0.011285905	0
1.790471296	0.019353945	0.010149546	2.64015998	0.012413721	0
1.766712843	0.020779571	0.023284253	2.6997721	0.01383021	0
1.74079453	0.022205433	0.037613024	2.75268865	0.015247433	0
1.722435726	0.023630467	0.047762571	2.78400661	0.016667023	0
1.693277624	0.025056684	0.063882438	2.83778711	0.017965566	0
1.693277624	0.026479706	0.063882438	2.89221557	0.019572359	0
1.637769238	0.027505622	0.09456989	2.92516885	0.019849596	0
1.574485358	0.028390087	0.129555973	2.9393869	0.019927689	0
1.528768334	0.030055289	0.154830333	2.83908303	0.02247166	0.03412408
1.520488873	0.031479219	0.159407579	2.72800455	0.023229225	0.07191376
1.504289928	0.032988719	0.168363061	2.6781735	0.024742412	0.08886663
1.453533232	0.03409543	0.196423572	2.62849674	0.025933707	0.10576701
1.418759496	0.034787034	0.215648006	2.57666011	0.02759958	0.12340219
1.414655763	0.036234223	0.217916728	2.56802068	0.029023549	0.12634139
1.413575833	0.037657363	0.218513761	2.52028778	0.029764008	0.14258045
1.402776536	0.039081569	0.224484082	2.50538475	0.031164946	0.14765057
0.1	0.06	0.8	2.48702595	0.03258998	0.15389636
			2.42994395	0.033527976	0.17331606
			2.38443263	0.034972926	0.18879933
			2.31747699	0.036403286	0.21157811
			2.27859952	0.037830568	0.22480449
			2.22568296	0.039259389	0.24280708
			2.18464563	0.040686908	0.25676826
			2.14036852	0.042114782	0.27183165
			2.14144845	0.043537686	0.27146425
			2.10905056	0.044964258	0.28248624
			2.05937379	0.046392724	0.29938662
			2.0161766	0.04805765	0.31408261
			2.00645723	0.049007396	0.3173892
			0.1	0.06	0.8

Table A. Compressive Stress-Strain Values

Reinforced by Carpet fibers, $E_c=71\text{MPa}$			Reinforced by Straw fibers, $E_c=183\text{MPa}$		
Stress(σ_c)(MPa)	Inelastic Strain (ϵ_c^{in})	Damage (d_c)	Stress(σ_c)(MPa)	Inelastic Strain (ϵ_c^{in})	Damage (d_c)
0.826364063	0	0	1.45893288	0	0
0.890581311	0.001471042	0	1.50493789	0.001391125	0
0.897986543	0.002723845	0	1.58852444	0.002212061	0
0.983763816	0.004182642	0	1.6905778	0.003030973	0
1.10903566	0.005987219	0	1.75699348	0.003498035	0
1.195862007	0.007163555	0	1.84252391	0.004081588	0
1.280906471	0.008488318	0	1.98539861	0.005133196	0
1.365518962	0.009398081	0	2.08745196	0.00585724	0
1.436686329	0.010457548	0	2.16391098	0.006512938	0
1.448306372	0.011808145	0	2.25484106	0.007119616	0
1.453911207	0.013153473	0	2.33885959	0.007727051	0
1.46217267	0.014427358	0	2.44099394	0.00858153	0
1.402776536	0.016271937	0.040621832	2.4999851	0.01005738	0
1.407096255	0.017694485	0.037667517	2.57434598	0.011285905	0
1.413575833	0.019116797	0.033236045	2.64015998	0.012413721	0
1.402776536	0.020185247	0.040621832	2.6997721	0.01383021	0
1.366058927	0.02192852	0.065733511	2.75268865	0.015247433	0
1.329341317	0.023671793	0.090845189	2.78400661	0.016667023	0
1.292623708	0.025415065	0.115956867	2.83778711	0.017965566	0
1.255906098	0.027158338	0.141068545	2.89221557	0.019572359	0
1.219188489	0.028901611	0.166180223	2.92516885	0.019849596	0
1.182470879	0.030644884	0.191291902	2.9393869	0.019927689	0
1.14575327	0.032388157	0.21640358	2.83908303	0.02247166	0.03412408
1.10903566	0.034131429	0.241515258	2.72800455	0.023229225	0.07191376
0.1	0.035	0.8	2.6781735	0.024742412	0.08886663
0.826364063	0	0	2.62849674	0.025933707	0.10576701
0.890581311	0.001471042	0	2.57666011	0.02759958	0.12340219
0.897986543	0.002723845	0	2.56802068	0.029023549	0.12634139
0.983763816	0.004182642	0	2.52028778	0.029764008	0.14258045
1.10903566	0.005987219	0	2.50538475	0.031164946	0.14765057
1.195862007	0.007163555	0	2.48702595	0.03258998	0.15389636
			2.42994395	0.033527976	0.17331606
			2.38443263	0.034972926	0.18879933
			2.31747699	0.036403286	0.21157811
			2.27859952	0.037830568	0.22480449
			2.22568296	0.039259389	0.24280708
			2.18464563	0.040686908	0.25676826
			2.14036852	0.042114782	0.27183165
			2.14144845	0.043537686	0.27146425
			2.10905056	0.044964258	0.28248624
			2.05937379	0.046392724	0.29938662
			2.0161766	0.04805765	0.31408261
			2.00645723	0.049007396	0.3173892
			0.1	0.06	0.8

Table C. Tensile Stress-Strain Values

Plain, and Tire, Carpet and Straw Fibers Reinforced		
Direct Tensile, $E_t=72\text{MPa}$		
Stress (σ_c) (MPa)	Cracking Strain (ϵ_t^{cr})	Damage (d_t)
0.4	0	0
0.32	0.00222	0.2
0.12	0.015	0.7
0.1	0.02083	0.75
0.06	0.02972	0.85
0.04	0.03278	0.9

Table D. Plasticity Parameters

Dilation Angle	Eccentricity	fb0/fc0	K	Viscosity Parameter
10	0.1	1.16	0.67	0.001

HOW TO CITE THIS ARTICLE

F. Faghih-Khorasani, M. Zaman-Kabir, Kh. Ghavami, A mathematical model for predicting complete compressive stress-strain curve of plain and short fiber reinforced clay adobes, AUT J. Civil Eng., 5(1) (2021) 37-68.

DOI: [10.22060/ajce.2021.17393.5629](https://doi.org/10.22060/ajce.2021.17393.5629)

